A NEW APPROACH TO DESIGNING THE OPTIMUM ACID TREATMENT FOR SANDSTONE RESERVOIRS

A Thesis

by

SHERIF SAYED ABDELMONEIM MAHMOUD

Submitted to the Office of Graduate and Professional Studies of
Texas A&M University
in partial fulfillment of the requirements for the degree of

MASTER OF SCIENCE

Chair of Committee,	Hisham A. Nasr-El-Din
Committee Members,	Robert Lane
	Mahmoud El-Halwagi
Head of Department,	A. Daniel Hill

August 2014

Major Subject: Petroleum Engineering

ABSTRACT

Since the early days, various acid types have been developed along with additives to help make acidizing more effective. Hydrofluoric acid (HF), unlike other acids, has a specific reactivity with silica which makes it more effective for use with sandstone reservoirs. Despite the significant advancements made in the area of acidizing, the success rate of treatments remains low with some companies reporting failure in 25 to 30% of treatments.

There have been great efforts in developing a systematic method for designing matrix acidizing treatments. Previous guidelines have highlighted the main factors affecting the treatment design to be mineralogy, permeability, and temperature. In this study our goal was to integrate the past experiences highlighted in the literature, the previously developed advisory systems, and the practical experiences of the research team to develop new software that can help design acid treatments.

A comprehensive examination of sandstone acidizing chemistry, previous guidelines, and practical experiences in the literature show that the HF concentration significantly controls the output of the treatment. It is clear that previous guidelines have emphasized the importance of using lower HF concentrations with the increase of mineral content. This hypothesis was represented graphically and experiments were designed to investigate its accuracy. Results show that these curves present a useful tool for better designing field treatments.

DEDICATION

I dedicate this thesis to my dad, mom, and brothers for their continuous support and encouragement.

ACKNOWLEDGEMENTS

I would like to express my deepest gratitude and appreciation to my committee chair, Dr. Hisham A. Nasr-El-Din, for his continuous encouragement, guidance, and support throughout the course of this research. I would like to extend my appreciation to Dr. Robert H. Lane and Dr. Mahmoud El-Halwagi for serving as committee members.

I would also like to thank all of my friends and colleagues in my research group, and the department faculty and staff for making my time at Texas A&M University a great experience. I also want to express my gratitude to Saudi Aramco for providing financial support during my education.

Last but not least, I want to thank my father and mother for their encouragement, patience, and love.

TABLE OF CONTENTS

LIST OF FIGURES

Page

LIST OF TABLES

Page

CHAPTER I

INTRODUCTION AND LITERATURE REVIEW

Stimulating wells with acid was first reported in 1896 (Walker et al. 1991). The aim of the acid job is to bypass the near wellbore damage and restore the well productivity. Unlike other acids, hydrofluoric acid (HF) has a special ability to react with silica and silicates which makes it a fundamental component in sandstone acidizing treatments. To achieve the goal of acidizing the reaction products should be maintained in solution. HF by itself is a weak acid, which means it is not capable of keeping reaction products in solution. In 1935, mud acid was introduced to the petroleum industry (Smith and Hendrickson 1965). The mud acid is composed of both HF and hydrochloric acid (HCl). Mud acid has been widely used in stimulation treatments ever since. However, despite the significant advancements made in the area of acidizing, the success rate of treatments has remained fairly low. Nitters et al. (2000) stated that some companies report failure in 25 to 30% of treatments.

Unlike carbonate acidizing, sandstone acidizing is complicated and until this day, its reactions remain not fully understood. Each different type of minerals has different structures, elements, surface area, and sensitivity to acids. This makes designing acid treatments more challenging. Material incompatibilities, chemical interaction, physical restrictions, and cost considerations build a great deal of complexity into the designs (Chiu et al. 1993). The low success rates and the highly complicated reaction makes it essential to have a systematic method for designing sandstone treatments.

Reactions in Sandstone Reservoirs

The key to success is to know how the formation minerals will respond to the acid used in the treatment and to anticipate how the spent acid will react as it invades deeply into the formation (McLeod 1984). The acid design and selection of solvents should prevent or reduce incompatibilities and potential damaging mechanisms.

The dissolution reaction of all aluminosilicate minerals in sandstones follows the following equations for the basic lattice atoms (Si and Al) concerned:

Kaolinite Clay

$$Al_4Si_4O_{10}(OH)_8 + 4(n+m)HF + \big(28 - 4(n+m)\big)H_3O^+ \rightarrow 4AlF_n^{(3-n)+} +$$

$$4SiF_m^{(4-m)-} + \big(46 - 4(n+m)\big)H_2O$$

Sodium or Potassium Feldspar

$$MAlSi_3O_8 + (n+3m)HF + (16 - n - 3m)H_3O^+ \rightleftharpoons$$

$$M^+ + AlF_n^{(3-n)+} + 3SiF_m^{(4-m)-} + (24 - n - 3m)H_2$$

where $0 \leq n < 6$, and $m = 4$ or 6

A comprehensive examination of sandstone acidizing chemistry is essential for evaluating and designing acid treatments. HF is the only common, inexpensive mineral acid able to dissolve siliceous minerals. For any acid system to be capable of damage removal, it should contain HF in some form.

Reactions of HF with Carbonates

One of the potential damaging mechanisms expected in sandstone acidizing is the reaction of carbonates with the HF. When HF reacts with carbonates it forms solid

calcium fluoride (CaF_2) in limestone and both calcium fluoride and magnesium fluoride (MgF_2) in dolomite (Kalfayan 2008).

$$2HF + CaCO_3 \rightarrow CaF_2 + H_2O + CO_2$$

$$4HF + CaMg(CO_3)_2 \rightarrow CaF_2 + MgF_2 + 2H_2O + 2CO_2$$

To avoid this precipitation reaction, a preflush of HCl or an organic acid is pumped ahead of the HF acid stage to dissolve the calcium based minerals. More details regarding the design of the preflush will be covered later.

Reactions with Iron Oxides

Metallic ions, such as Na, K, Mg, Ca, and Fe, which are in the minerals constituting the rock as substitution cations in the lattice or as exchangeable (adsorbed) cations, come into solution as free ions during the reaction. In the case of iron, iron oxides are present in the formation in several forms as FeO, Fe_2O_3, and Fe_3O_4. The presence of iron oxides in the formation will result in fluorinated complexes ($FeF_z^{(3-z)+}$, where $1 < z < 3$) also being formed through reactions similar to those for aluminum.

This mechanism of forming iron fluorine complexes applies only to relatively clean sandstones. In the presence of clays, the dissolved aluminum ions have a greater affinity for fluorine than iron does. Therefore, the iron fluorine complexes do not form and iron hydroxide still precipitates at pH levels greater than 2.2 (Economides and Nolte 2000).

Problems caused by iron oxides will be addressed by the use of preflush and by using iron control agents, which will be discussed with more details in the additives section.

Reactions with Sodium and Potassium Feldspars

The aluminum or silicon fluorine complexes react with alkali ions released in the solution from highly substituted clays or alkali feldspars as soon as their concentration becomes sufficiently high to form insoluble alkali fluosilicates and, probably, fluoaluminates (Economides and Nolte 2000).

$$2Na^+ + SiF_6{}^{2-} \rightleftharpoons Na_2SiF_6$$

$$2K^+ + SiF_6{}^{2-} \rightleftharpoons K_2SiF_6$$

$$3Na^+ + AlF_3 + 3F^- \rightleftharpoons Na_3AlF_6$$

$$2K^+ + AlF_4{}^- + F^- \rightleftharpoons K_2AlF_5$$

This represents another damaging mechanism in sandstone acidizing which is the precipitation of sodium or potassium hexafluosilicates (M_2SiF_6, where M = Na or K). This results from the reaction of cations in sodium and potassium feldspars with the products of the HF reaction with the formation. The reactions with feldspars are represented by the general formula shown below:

$$MAlSi_3O_8 + (n + 3m)HF + (16 - n - 3m)H_3O^+ \rightleftharpoons$$

$$M^+ + AlF_n{}^{(3-n)+} + 3SiF_m{}^{(4-m)-} + (24 - n - 3m)H_2O$$

where $0 \leq n < 6$, and m = 4 or 6

Reactions with Sodium and Potassium Salts

Similar to the reaction of feldspars, cations in formation brines will react with the spent HF acid resulting in the precipitation of sodium or potassium hexafluosilicates (M_2SiF_6, where M = Na or K).

To avoid this precipitation reaction, a preflush of acid or NH_4Cl is pumped ahead of the HF acid. The preflush displaces the formation brine away from the wellbore to prevent it from mixing with reacted mud acid and causing a damaging precipitate (McLeod 1984).

Clays and Minerals Reactions

Clays are layered silicates formed by the chemical weathering of other rock-forming silicate minerals. The layers are composed of various combinations of two fundamental units:

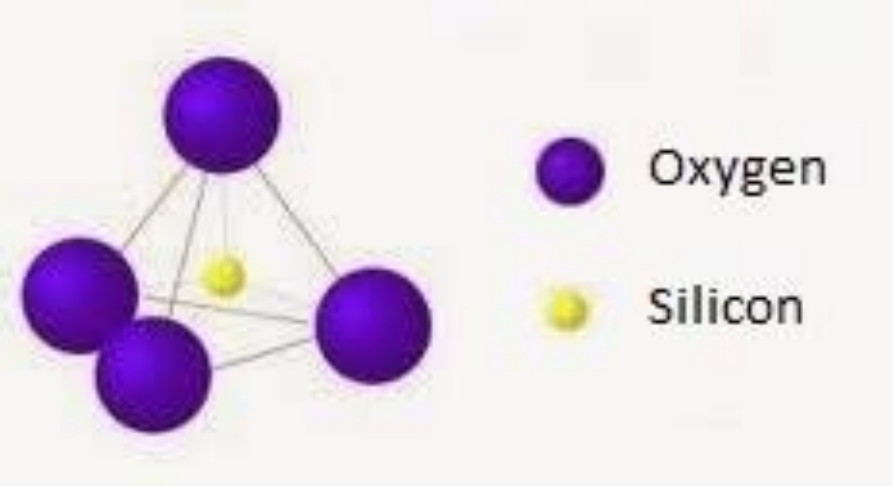

Figure 1.1 - Structure of the tetrahedral layer.

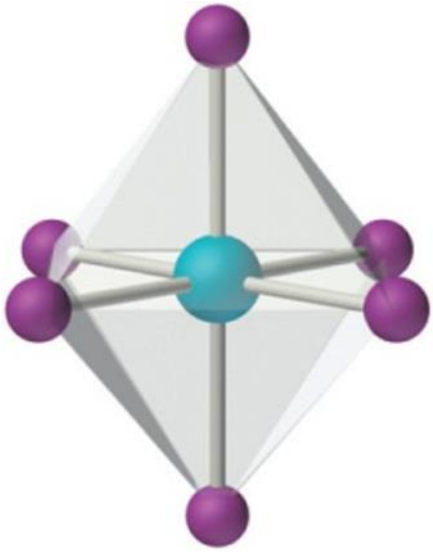

Figure 1.2 - Structure of the octahedral layer (Averill and Eldredge 2012).

1. Tetrahedral layers consisting of linked silicon-oxygen tetrahedra (**Fig. 1.1**).
2. Octahedral layers in which hydroxyl ions occur in two planes, one above and one be``low a plane of magnesiun or aluminum ions (**Fig. 1.2**).

Each clay mineral has a specific arrangement of the two fundamental units. Three-layer clay would have one octahedral sheet with tetrahedral sheets on each side. A pure crystal of this type is known as the clay mineral pyrophyllite. In this case, some of the aluminum in the octahedral layer is substituted with magnesium and/or ferrous iron and, in some instances, a small amount of silicon in the tetrahedral layer is substituted by aluminum. The clay mineral Smectite is formed (Simon and Anderson 1990).

Kaolinite is a two-layer clay that consists of one silica tetrahedral sheet and one alumina octahedral sheet. There is essentially no isomorphous substitution in the crystal lattice. The lack of isomorphous substitution makes kaolinite very stable from a

chemical point of view (Simon and Anderson 1990). Kaolinite is considered the most detrimental from the fines migration standpoint.

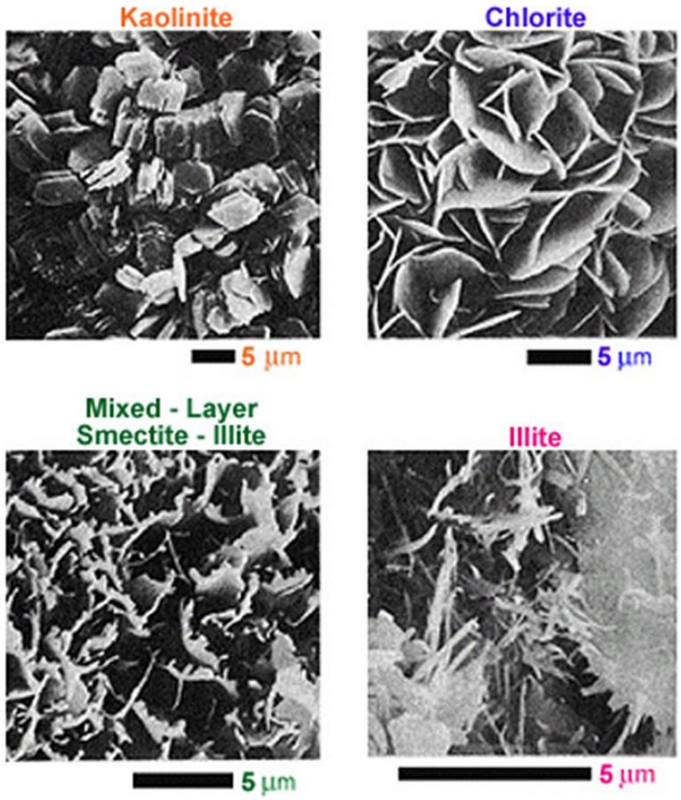

Figure 1.3 - SEM picture of different clays showing the variations in morphology (Wilson 1982).

Illite is similar to Smectite in structure but has a greater degree of isomorphous substitution, particularly in the silica tetrahedral layer. Chlorites are a family of clay minerals that consist of stacked mica-like (similar to illite) and brucite ($Mg_2(OH)_6$) layers with two layers of each type forming a unit cell. There is generally a high degree of aluminum substitution in the tetrahedral layer and iron and magnesium substitution in the octahedral layers of chlorite clays. Different clay structures can be seen in **Fig. 1.3.**

Zeolite minerals are sensitive to HCl and strong mineral acids. Several core studies have shown that the use of HCl alone causes significant damage, whereas weak organic acids reduce the damage (McLeod and Norman 2000). Zeolites are inherently more unstable because of their open structure that can allow the acid to penetrate inside the crystal (Hartman et al. 2006).

Secondary and Tertiary Reactions

The primary reaction results in complete dissolution of the aluminosilicate and is the only reaction that provides permeability improvement or removes clay damage (Gdanski 1998).

$$(5+\mathrm{n})\mathrm{HF} + \mathrm{M}-\mathrm{Al}-\mathrm{Si} + (3-\mathrm{n}+1)\mathrm{H}^{+} \rightarrow \mathrm{HSiF_5} + \mathrm{M}^{+} + \mathrm{AlF_n}^{(3-\mathrm{n})+} + \mathrm{Water}$$

The secondary reaction is the reaction of fluosilic acid resulting from the primary reaction with the aluminosilicates. At temperatures below 125°F, the rate of secondary reactions is very slow, but above this temperature the secondary reaction becomes very fast and continues to completion (Gdanski 1999). The damage resulting from the secondary reactions becomes very significant in formations of high K-Feldspar content or at temperatures of higher than 300°F (Gdanski 1998). This reaction could be represented by the following general formula:

$$(\mathrm{n}/5)\mathrm{HSiF_5} + \mathrm{M}-\mathrm{Al}-\mathrm{Si} + (3-n+1)\mathrm{H}^{+} + \mathrm{Water} \rightarrow \mathrm{AlF_n}^{(3-\mathrm{n})+} + \mathrm{M}^{+} + \mathrm{Silica\ Gel}$$

The tertiary reaction continues to reduce the F/Al ratio in the spent HF until all HCl is consumed. The tertiary reaction could be represented with this general formula:

$$\mathrm{AlF_2}^{+} + \mathrm{M}-\mathrm{Al}-\mathrm{Si} + (3+1)\mathrm{H}^{+} \rightarrow 2\mathrm{AlF}^{2+} + \mathrm{M}^{+} + \mathrm{Silica\ Gel}$$

Previous Guidelines

In 1984, McLeod presented guidelines for designing acid treatments. McLeod's work was the first to emphasize the effect of the reservoir mineralogy on the outcome of the acid treatment (McLeod 1984). His guidelines could be summarized in **Table 1.1**. The guidelines were presented in two sets. The first set was designed for low permeability reservoirs (permeability less than 10 md). The second set handles high permeability reservoirs (permeability more than 100 md).

Table 1.1 - McLeod's guidelines for sandstone acidizing.

High permeability (100 md or more)	
High quartz (80%), low clay (<5%)	12% HCl and 3% HF
High feldspar (>20%)	13.5% HCl and 1.5% HF
High clay (>10%)	6.5% HCl and 1% HF
High iron chlorite clay	3% HCl and 0.5% HF

Low permeability (10 md or less)	
Low clay (<5%)	6% HCl and 1.5% HF
High chlorite	3% HCl and 0.5% HF

McLeod's guidelines, despite having their drawbacks, became very popular. The major disadvantages were the fact that it neglected the formations with permeability between 10 and 100 md, temperature effect, and mineral sensitivity except for chlorite.

Since then, extensive research has been reported since on the topic of mineral sensitivity. Simon and Anderson (1990) studied the sensitivity of chlorite in different acids (Simon and Anderson, 1990). In HCl, chlorite becomes unstable and aluminum (Al) and iron (Fe) are leached from clays leaving an amorphous silica gel which causes

damage to the formation. **Table 1.2** shows the ions leached from chlorite after 120 hours at a temperature of 180°F. **Fig. 1-4** shows the percent of chloride destroyed by different acids. The tests show that in the presence of chlorite, HCl should be avoided. Formic acid, does not completely destroy chlorite, but it still should be avoided as it shows high reactivity with chlorite. On the other hand, chlorite seemed to be fairly stable in acetic acid even after 120 hours.

Table 1.2 - Ions leached from chlorite by various acids.

Fluid	Ionic Concentration (mg/l)					Amorphous Material	Percent Chloride Destroyed
	Mg	Al	Si	Ca	Fe		
DI Water	1	1	7	6	1	0%	0%
10% Acetic Acid	27	11	26	35	53	4%	30%
10% Formic Acid	158	214	110	73	460	35%	92%
3% HCl Acid	158	265	125	65	565	55%	100%

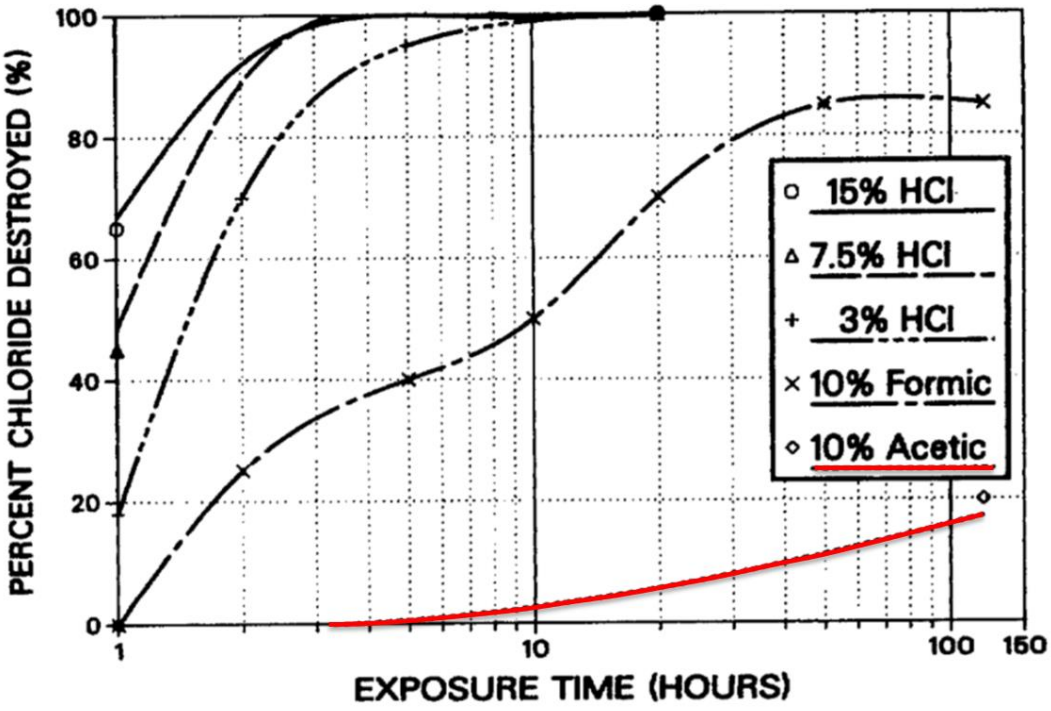

Figure 1.4 - Percent chloride destroyed by acid at 180°F.

Coulter and Jennings (1999) summarized the efforts done in the subject of mineral sensitivity with HCl. Studies have proven that all clays become unstable in HCl at different temperatures (Coulter and Jennings 1999). Stability temperatures of different clay minerals are summarized in **Table 1.3**.

Table 1.3 - Stability limit of clays in HCl.

Mineral	Temp, °F
Smectite and mixed layer	150
Chlorite	125
Illite	150
Kaolinite	> 200
Zeolite	75

Smectite and mixed layer clays are water swelling clays and are reactive to hydrochloric acid. They become unstable in HCl at temperatures higher than 150°F.

Chlorite typically has iron in its structure. When chlorite comes into contact with HCl, the iron is leached, disintegrating the structure and leaving an amorphous residue and iron in solution which precipitates when the pH of the fluid increases. Chlorite sensitivity to HCl starts at a temperature of 125°F.

Illite clays are very troublesome when using HF acid. Their structure typically contains potassium which, when dissolved, reacts with the HF–aluminosilicate reaction products, forming the insoluble potassium fluosilicate. Illite can also be troublesome since it often occurs as a needle-like structure making it susceptible to fluid retention and/or fines migration within the sandstone pore. When fines migration occurs, illite will accumulate at pore throats resulting in the plugging of these pore throats and dramatic decrease in the permeability. Illite instability in HCl begins at approximately 150°F.

Kaolinite clay is considered the most detrimental from a migration standpoint. It becomes unstable in HCl only at higher temperatures (>200°F).

Zeolites are secondary minerals, hydrated silicates of aluminum, calcium, sodium, and potassium. The significance of the zeolites is that they will either decompose and/or gelatinize in hydrochloric acid at temperatures rise above approximately 75°F.

Another important guideline outlined by Coulter and Jennings was that the maximum acceptable calcium carbonate concentration for HF acidizing should be less than 15–20%. This agrees with McLeod's guideline where he recommended the use of

only HCl for formations with an HCl solubility of 20% or higher. Coulter and Jennings, on the other hand, did not agree with McLeod in their definition of the most significant characteristics in designing sandstone treatments. McLeod considered permeability and mineralogy as the significant parameters for the design. Coulter and Jennings agreed on the importance of mineralogy but they emphasized the importance of temperature.

In the year 2000, Economides and Nolte published a book on reservoir stimulation. In the chapter on sandstone acidizing written by McLeod and Norman, they modified the original McLeod's guidelines. Their new guidelines are shown in **Table 1.4** (Economides and Nolte 2000). The guidelines have three sets: high, medium, and low permeability. In each set they proposed using three different concentrations, the highest for formations with low (<10%) clay and feldspar content. They proposed using the same fluid for formations that have either high (>10%) feldspar or high clay content. They used the lowest concentration for the formations that have high clay and feldspar contents.

Table 1.4 - McLeod and Norman guidelines.

Mineralogy	>100mD	20 to 100mD	<20mD
<10% silt and <10% clay	12% HCl and 3% HF	8% HCl and 2% HF	6% HCl and 1.5% HF
>10% silt and >10% clay	13.5% HCl and 1.5% HF	9% HCl and 1% HF	4.5% HCl and 0.5% HF
>10% silt and <10% clay	12% HCl and 2% HF	9% HCl and 1.5% HF	6% HCl and 1% HF
<10% silt and >10% clay	12% HCl and 2% HF	9% HCl and 1.5% HF	6% HCl and 1% HF

In addition to the guidelines shown in **Table 1.4**, McLeod and Norman also recommended replacing HCl with organic acid (acetic acid) for formations with chlorite and zeolite.

The updated guidelines proposed by McLeod and Norman covered two of the main limitations of McLeod's guidelines published in 1984; they added recommendations for medium permeability, and they considered the mineral sensitivity of two of the most troublesome minerals (chlorites and zeolites). However the temperature effect remains neglected in the recommendations.

The temperature effect on the acid concentration was also widely discussed in the literature. An example of how the HCl concentration should be varied with temperature is shown in **Table 1.5.** Based on the literature, the acid concentration should be decreased with increasing temperature due to the greater reactivity of the acids.

Table 1.5 - Effect of temperature on HF concentration.

Temperature	Maximum HCl Concentration, wt%	Maximum Mud Acid Strength, wt%
< 180°F	15	12% - 3%
180 – 220°F	10	9% - 3%
> 220°F	7.5	7.5% - 1.5%

Walsh et al. (1982) studied the HCl concentration in mud acid. They tested the effect of different HCl concentrations for different carbonate contents, and different HF concentrations during treatments. As shown in **Fig. 1-5**, they defined a maximum limit for the HF concentration given the HCl concentration and the carbonate content remaining after the preflush.

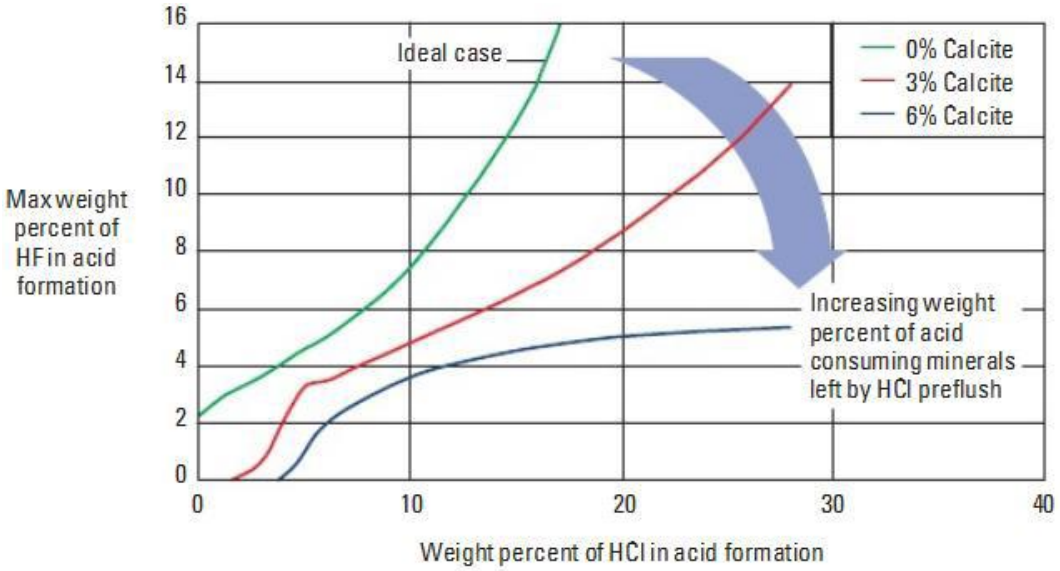

Figure 1.5 - Maximum HF concentration in mud acid.

CHAPTER II

NEW SANDSTONE DESIGN METHODOLOGY

Taking a close look at McLeod's 1984 guidelines, it could be clearly seen that the concentration of HF is decreased with the increase of both feldspar and clay content. For example, if we consider the high permeability set, the guidelines divide the mineralogy into three types (Fig. 2.1). Type 1 is the low clay and low feldspar formations, for this type McLeod recommended using full strength mud acid (3% HF). Type 2 represents the formations that have high feldspar content, for these formations McLeod recommended to decrease HF concentration to 1.5%. The cutoff value for the difference between low and high feldspar content was chosen to be 20%.

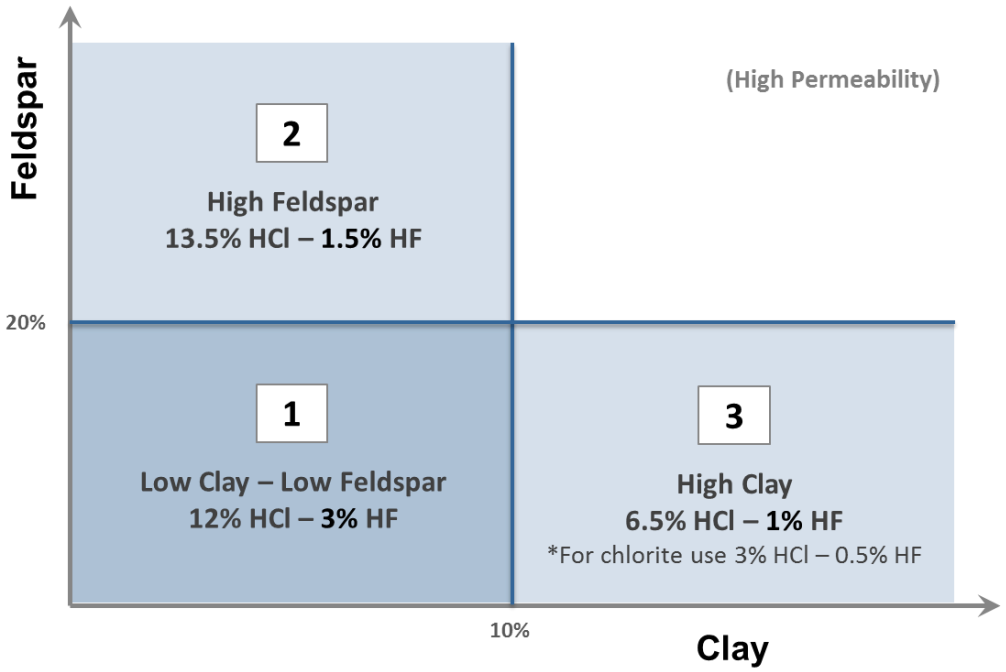

Figure 2.1 - High permeability guidelines by McLeod.

For the last type, the high clay, McLeod suggested using only 1% HF, which is less than even what he recommended for the high feldspar reservoirs, this implies that clay content has higher effect on the acid concentration. The same conclusion can be reached also from the fact that for clays he used a cutoff value of 10% percent instead of 20%. This could be explained by looking into the surface areas of both clays and feldspars. **Table 2.1** has a list of the surface areas of different sandstone minerals. This is also shown in **Fig. 2.2**. It is clear that clays have much higher surface areas than feldspars which make them more reactive and so their concentration will affect the acid design more than feldspars. Quartz on the other hand has a very small surface area which is why its reaction with acids could be completely ignored.

Table 2.1 - Relative surface area of sandstone minerals (McLeod and Norman 2000)

Mineral	Surface Area
Quartz	<0.1 cm^2/g
Feldspar	few m^2/g
Kaolinite	15-30 m^2/g
Smectite	82 m^2/g
Illite	113 m^2/g

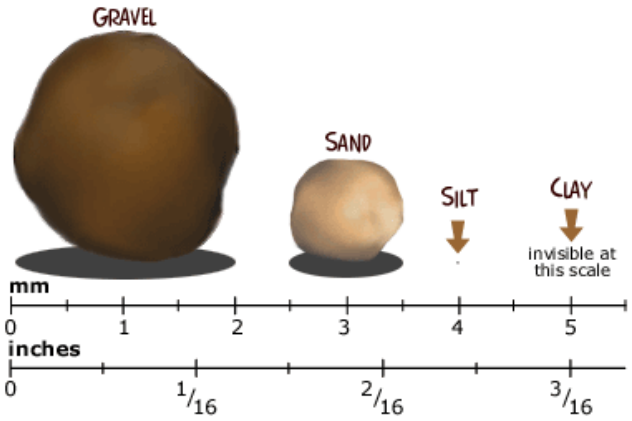

Figure 2.2 - Size of different sandstone minerals

In 2000, when McLeod and Norman updated the guidelines, they modified the old guidelines by adding the medium permeability set (between 20 and 100 md) and they also added some guidelines for the formations containing chlorite and zeolites. **Fig. 2.3** shows the updated guidelines.

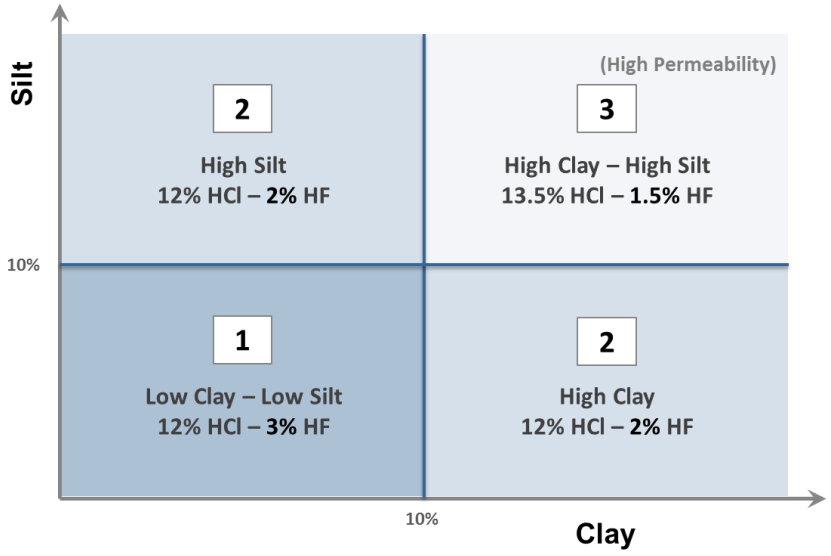

Figure 2.3 - McLeod and Norman guidelines for high permeability formations.

The updated guidelines still had the same idea of decreasing the HF concentration as the mineral content was increased. The major difference in the new guidelines was they added guidelines for zeolites and chlorites which were also following the rule of decreasing the HF concentration as the amount of chlorites and zeolites increased. Once again, this would agree with the fact that both zeolites and chlorites have bigger relative surface area than that of most of the other clay minerals. Another difference, unlike in the original guidelines, the guidelines used the same cutoff value for both clays and silt. Guidelines also proposed using the same acid for both high clay formation and high silt formation.

After 2000, several studies were published discussing the type of acid to use in different cases, but there was no updated guidelines to designing acid treatments. All guidelines published were regarding one formation or one specific type of acid. Successful sandstone treatments were reported in many papers in the literature. The reported treatments, while they might be different than that proposed by McLeod and Norman, all followed the same trend of using low HF concentrations for formation with high content of both clays and feldspars. The trend was represented graphically as shown in **Fig. 2.4**. The concentration of HF should be decreased as mineral content increase where clays have the more significant effect due to their higher relative surface area.

Data was collected from the literature and filtered to include only formation that are in the medium permeability range (10 to 100 md) and in a temperature range of 200 to 250°F. Successful treatments were sorted based on their HF concentration. This provided a guideline to better tune the proposed relation between the HF concentration

and the mineral composition. The final curves shown in **Fig. 2.4** represent the concentration of the HF in the acid that is able to achieve the best results based on the mineralogy. These curves were proposed to be used to design acid treatments.

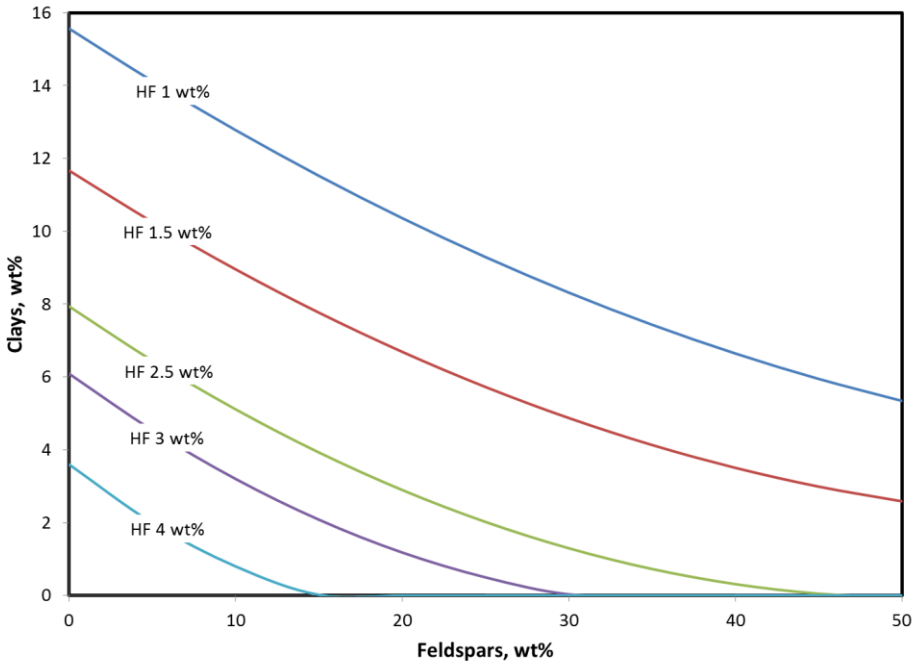

Figure 2.4 - Optimum HF concentration based on reservoir mineralogy.

Fig. 2.4 only determines the concentration of HF in the mud acid. For determining HF concentration, the work by Walsh et al. was reconstructed as shown in **Fig. 2.5**. Based on the proposed HF concentration and the carbonate content expected to be remaining after the preflush, the minimum HCl concentration was identified using **Fig. 2.5**.

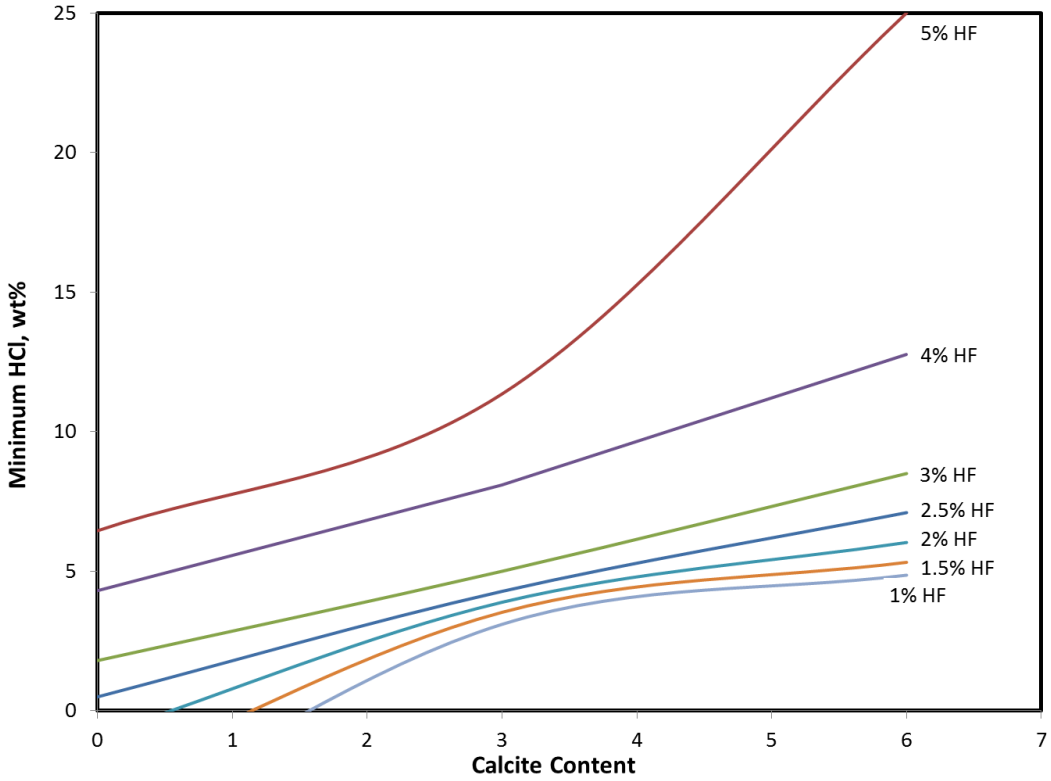

Figure 2.5 - Minimum HCl requirement for mud acid treatments.

For the design of organic mud acid treatments, a comparison between the HCl and potential organic acids that replace HCl in acid formulation had to be used. The work published by Williams et al. (1979) compared the dissolving strength of HCl, acetic acid, and formic acid. Their work was compared and compositions of the three acids showing the same dissolving power were identified. Then, these compositions were compared and a correction factor was calculated to represent the ratio of the concentration of the desired acid to its equivalent HCl concentration. The correction factor for both acetic and formic acids was plotted versus the HCl concentration and is shown in **Fig. 2.6**. This figure can be used when designing organic mud acid treatments

where the HCl concentration obtained from **Fig. 2.5** will be used to determine the correction factor for this design. Then, the concentration of the organic acid can be calculated by multiplying the correction factor by the calculated HCl concentration.

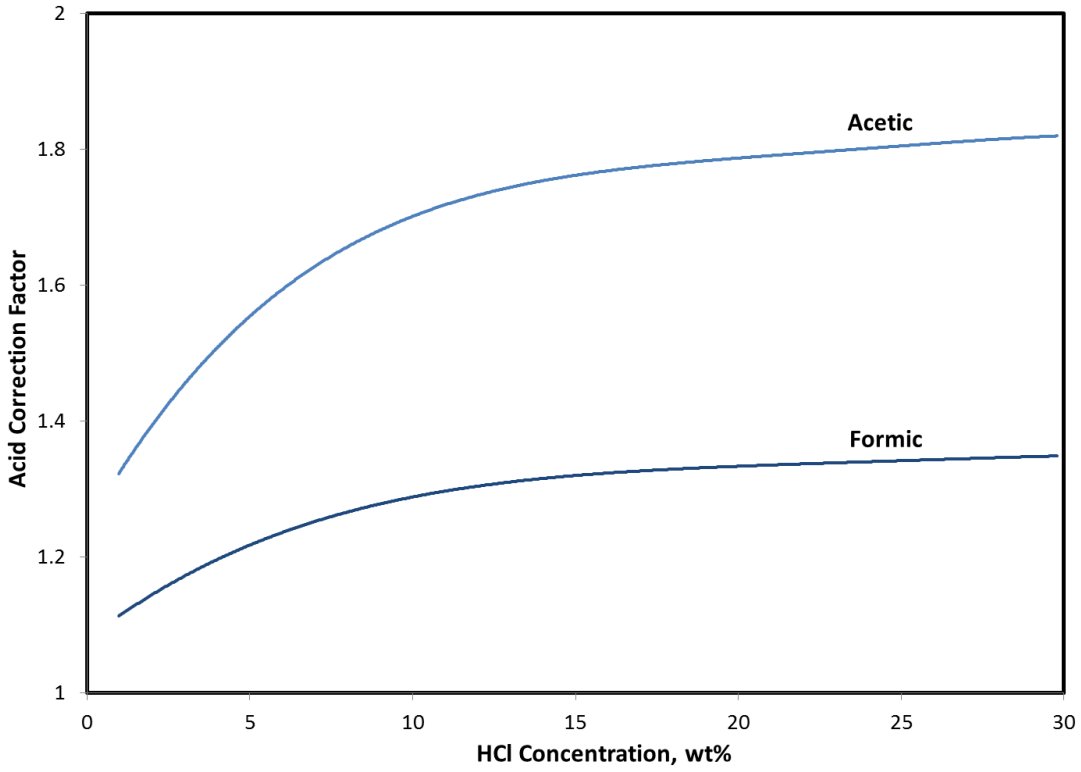

Figure 2.6 - Organic acid correction factor.

CHAPTER III

EXPERIMENTAL STUDY

The objective of the experimental work is to verify the design methodology explained in the previous chapter. This will be done by experimentally identifying the optimum acid concentration for different types of sandstone cores though a series of coreflood experiments.

Materials

Acids

The acid solutions were prepared using 36.5 wt% HCl, ammonium bifluoride (ABF), corrosion inhibitors A270 and A262 were used for HCl and HF acids, respectively.

Cores

The cores used were Bandera and Grey Berea sandstone. All cores had a diameter of 1.5 inch and length of 6 inch.

Brine

The brine used was 5 wt% ammonium chloride (NH_4Cl). The deionized water, used throughout the experiments, was obtained from a purification water system that has a resistivity of 18.2 MΩ.cm at room temperature.

Equipment

Coreflood

The coreflood setup used in the experiments is shown in **Fig. 3.1**. A back pressure of 1200 psi was applied to all experiments to keep the CO_2, resulting from dissolution of carbonates, in solution. The overburden pressure applied was 1800 psi. A pressure transducer of the range 0-300 psi was used for all experiments. Pressure transducers were connected to a computer to monitor and record the pressure drop across the core during the experiments. A Teledyne ISCO D500 precision syringe pump, that has a maximum allowable working pressure of 2000 psi, is used to inject the treatment into the core.

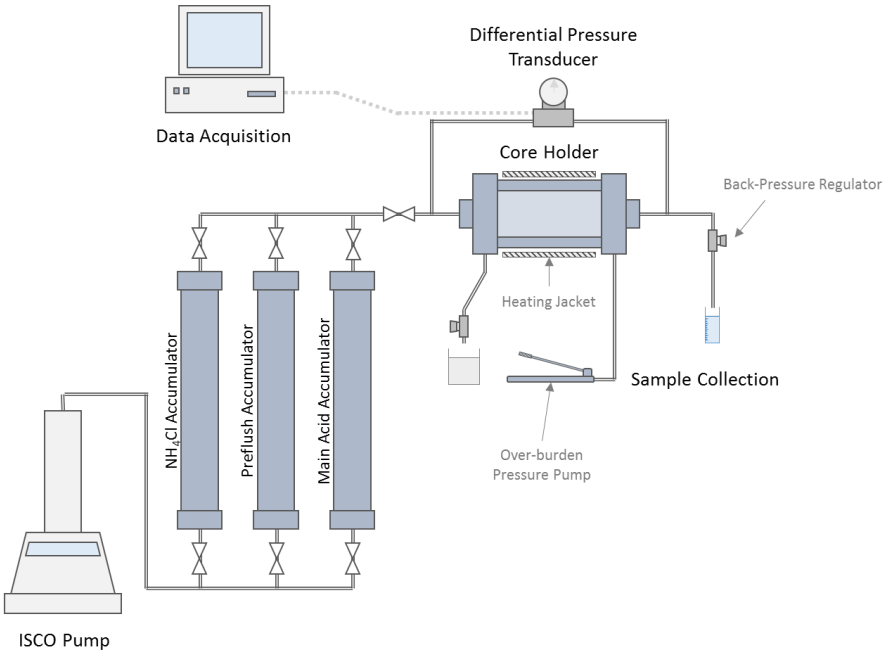

Figure 3.1 - The coreflood setup

Inductively Coupled Plasma (ICP)

Optical emission spectroscopy (OES) uses quantitative measurements of the optical emission from excited atoms to determine analyte concentration. Analyte atoms in solution are aspirated into the excitation region where they are desolvated, vaporized, and atomised by a plasma. Electrons can be in their ground state (unexcited) or enter one of the upper level orbitals when energy is applied to them. This is the excited state. A photon of light is emitted when an electron falls from its excited state to its ground state. Each element has a unique set of wavelengths that it can emit. An illustration is given in **Fig. 3.2**.

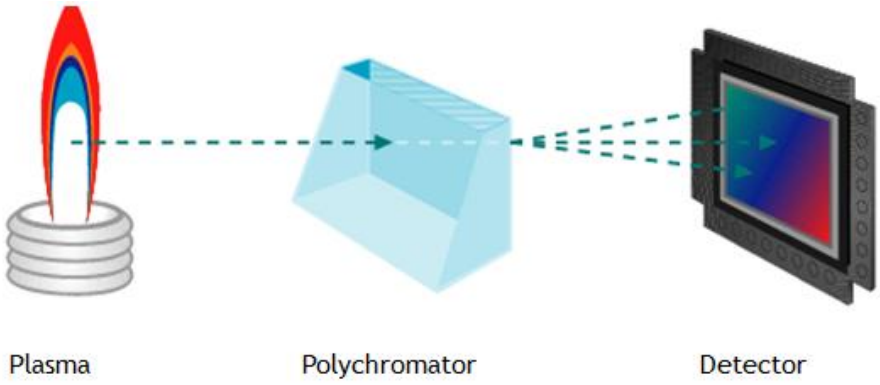

Fig. 3.2 - An illustration of ICP theory.

An Optima 7000 ICP-OES Spectrometer (**Fig. 3.3)** was used to analyze core effluent samples for all coreflood experiments.

Fig. 3.3 - Optima 7000 ICP-OES Spectrometer

Outline of Experimental Work

Summary of Experiments

The experiments are designed to confirm the design methodology previously explained. Two types of sandstones were used for this objective: Bandera and Grey Berea. Based on the mineralogy of Bandera it could be concluded that the optimum HF concentration should be around 1%. For this reason the following experiments were designed:

Six Coreflood Experiments on Bandera SS

- Temp: 280°F
- Rate: 5 cc/min
- HCl concentration in all experiments: 9 wt%

- HF concentrations tested will be 0, 0.5, 1, 1.5, 2.5, and 3 wt%

For the Grey Berea cores, it could be concluded that the optimum HF concentration should be around 2%. For this reason the following experiments were designed:

Four Coreflood Experiments on Grey Berea SS

- Temp: 280°F
- Rate: 5 cc/min
- HCl concentration in all experiments: 9 wt%
- HF concentrations tested will be 1, 1.5, 2, and 2.5 wt%

Core Preparation

Cores were dried in the oven at 250°F for 12 hours and the dry weight of the cores was measured. Then cores were saturated with 5 wt% NH_4Cl under vaccum. The weight of the saturated core was obtained after the measurement of the initial permeability to ensure that the core is completely saturated. The difference between the dry weight and the weight of the saturated cores was used to calculate the porosity of the cores.

$$V_p = \frac{W_{wet} - W_{dry}}{\rho}$$

where:

V_p: pore volume, cm^3; ρ: brine density, g/cm^3

Initial and final permeability measurements were performed seperately from the acid injection. Permeability was measured at room temperature by injecting a 5 wt%

NH_4Cl brine. Darcy's equation for laminar flow was used for the permeability calculation:

$$k = 122.8\frac{qL\mu}{\Delta p\, d^2}$$

where:

k: permeability, md; L: core length, inch, d: core diameter, inch; q : flow rate, cm^3/min; μ: dynamic viscosity, cp; Δp: psia

Acid Preparation

Mud acid was prepared using ABF and HCl. The HCl reacts with the ABF forming HF and NH_4Cl. The equation for this reaction is shown below.

$$HCl + NH_4HF_2 \rightarrow NH_4Cl + 2HF$$

An example of solution preparation is 9 wt.% HCl 1 wt.% HF:

To prepare 100 g of the solution:

Weight of HF = $\frac{1}{100} \times 100 = 1$ g

Number of moles of HF = $\frac{1}{20.01} = 0.04998$ g.moles

Number of moles of HCl required to form HF = $\frac{0.04998}{2} = 0.02499$ g.moles

Weight of pure HCl required to form HF = $0.02499 \times 36.46094 = 0.9111$ g

Weight of pure HCl (9%) = $\frac{9}{100} \times 100 = 9$g

Total Weight of pure HCl = $9 + 0.9111 = 9.9111$g

HCl acid weight (36.5% purity) = $\frac{100}{36.5} \times 9.9111 = 27.154$g

Number of moles of ABF required to form HF = $\frac{0.04998}{2} = 0.02499$g.moles

Weight of ABF required to form HF = $0.02499 \times 57.04 = 1.425$g

1 wt.% of corrosion inhibitor is added (1g)

Finally, deionized water was added.

DI H_2O weight = 100 – (27.154+1.425+1) = 70.421g

Core Effluent Analysis

The core effluent analysis should include the following steps:

1. Make sure that the ventilation is working.
2. Open the air and argon tanks and adjust their pressures.
3. Switch the machine on.
4. Go to computer and select the method.
5. Light the lamp and leave it 30 min, to warm up.
6. Aspirate deionized water and select auto zero.
7. Aspirate the calibration blank (2% HNO3) and select auto zero.
8. Calibrate using standards (5, 15, and 30) ppm and check the linearity of the standard and the correlation coefficient value.
9. If everything is right, analyze samples.
10. Save the method and close the Winlab program window after closing air and argon and bleeding them from the pipes. The results will be in ppm.
11. If any samples are deviated from the range of the standard curve (0-30 ppm), make the appropriate dilution and reanalyze them again.

CHAPTER IV

EXPERIMENTAL RESULTS

The objective of the experimental work, as previously mentioned, is to verify the curves used to determine the optimum HF concentration. For this reason several HF concentrations were tested and compared based on the ratio of final to initial permeability. To make sure that the difference in output of the experiments will be only because of the mineralogy effect, all parameters had to be selected to match all experiments. For the preflush 5 pore volumes of 12% HF was used. That is because of the high dolomite content (16%) in Bandera sandstone cores (**Table 4.1**). For the main acid, 9 wt% of HCl was used to make sure that the HCl concentration was higher than the minimum requirement for all experiments done, so for that reason it was designed based on the experiment done using 3% HF on Bandera sandstone.

Table 4.1 - Mineral composition of sandstone cores.

Mineral	Grey Berea, wt%	Bandera, wt%
Quartz	86	57
Plagioclase	0	12
K-Feldspar	3	0
Mica/Illite	1	10
Kaolinite	5	3
Chlorite	2	1
Calcite	2	0
Dolomite	1	16

Bandera Sandstone Experiments

The Bandera sandstone cores were tested to identify the optimum HF concentration; six experiments were done using concentrations of 0, 0.5, 1, 1.5, 2.5, and 3 wt%. **Table 4.2** has a list of all experiments done using Bandera sandstone experiments.

Table 4.2 - Bandera sandstone experiments summary.

Core ID	HF Concentration, wt.%	Initial Permeability, md	Final Permeability, md	K_f/K_i
Ba-10	0	16.35	31.34	**1.917**
Ba-09	0.5	14.51	33.89	**2.336**
Ba-07	1	9.23	24.75	**2.680**
Ba-08	1.5	9.33	21.52	**2.307**
Ba-04	2.5	13.80	19.72	**1.429**
Ba-05	3	14.88	7.43	**0.499**

The first experiment was done using 0 wt% HF. A 5 pore volume of 12 wt% HCl was injected in the core followed by 5 pore volumes of 9 wt% of HCl as a main acid. By comparing the initial and final permeability (**Fig. 4.1 and Fig. 4.2**) an enhancement in the permeability was achieved despite the damage resulting from injecting HCl at that high temperature. From the ICP analysis (**Fig. 4.4**) it can be seen that the high iron content in the core effluent that is resulting from dissolving the chlorite which results in leaving an amorphous silica rich residue that damages the formation. Also the low ratio between the silicon to aluminum ions indicates the occurrence of secondary and tertiary

reactions. Finally, the spikes in the pressure curve (**Fig. 4.3**) are a result of the fines migration caused by injecting the HCl in an Illite rich formation. Despite the damaging mechanisms, the permeability enhancement proves that dissolving the carbonate content, which is the only mechanism enhancing the permeability, could be successful for formations with carbonate content of 15 to 20% as previously mentioned.

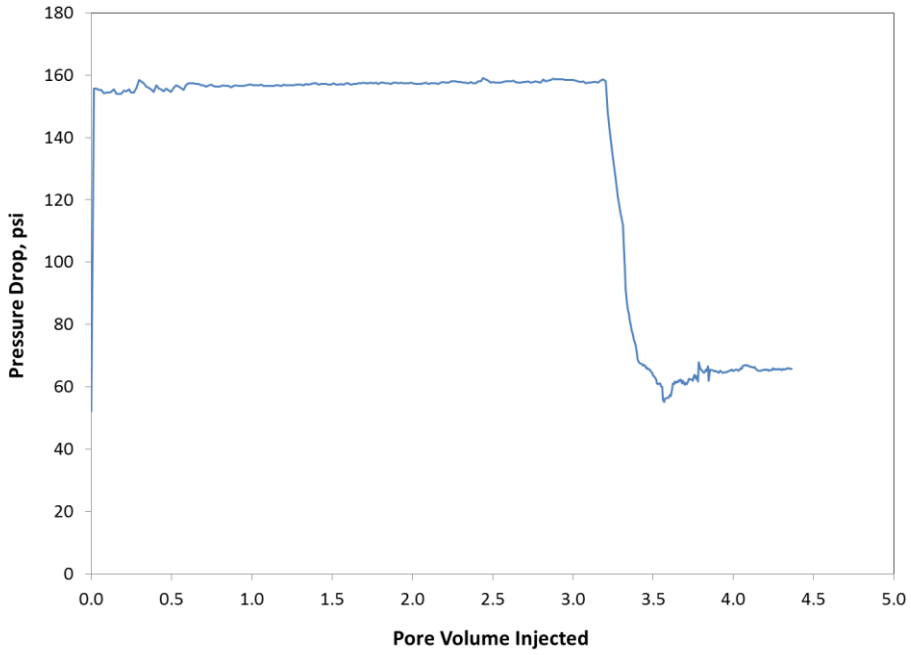

Figure 4.1 - Initial permeability for core Ba-10.

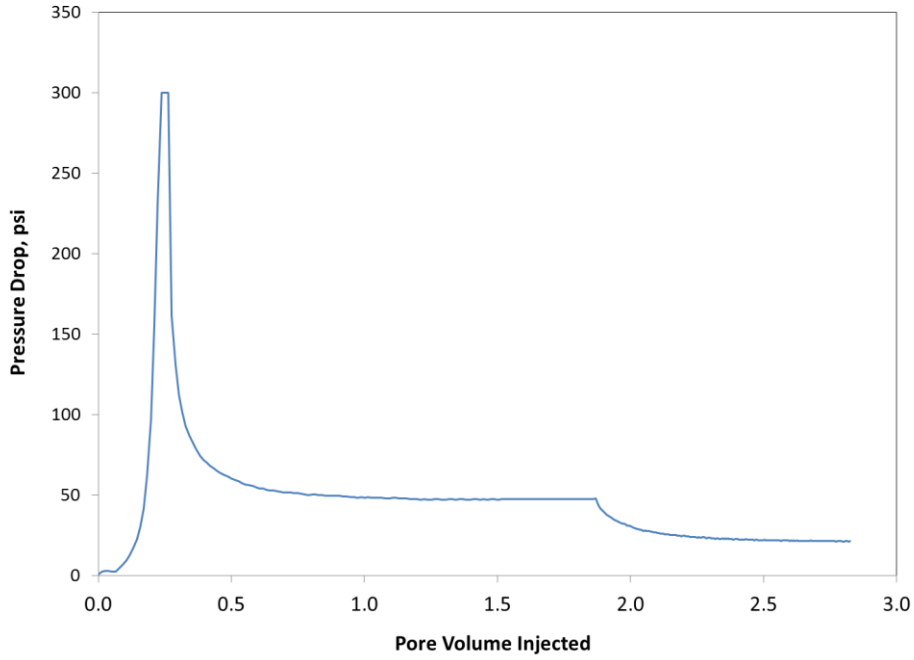

Figure 4.2 - Final permeability for core Ba-10.

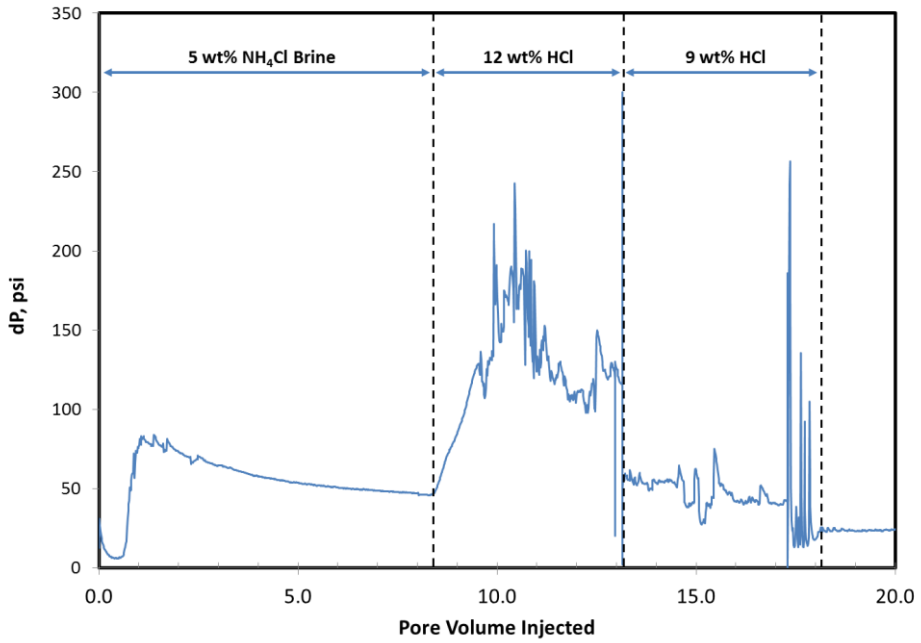

Figure 4.3 - Pressure drop curve during 0% HF experiment with Bandera core.

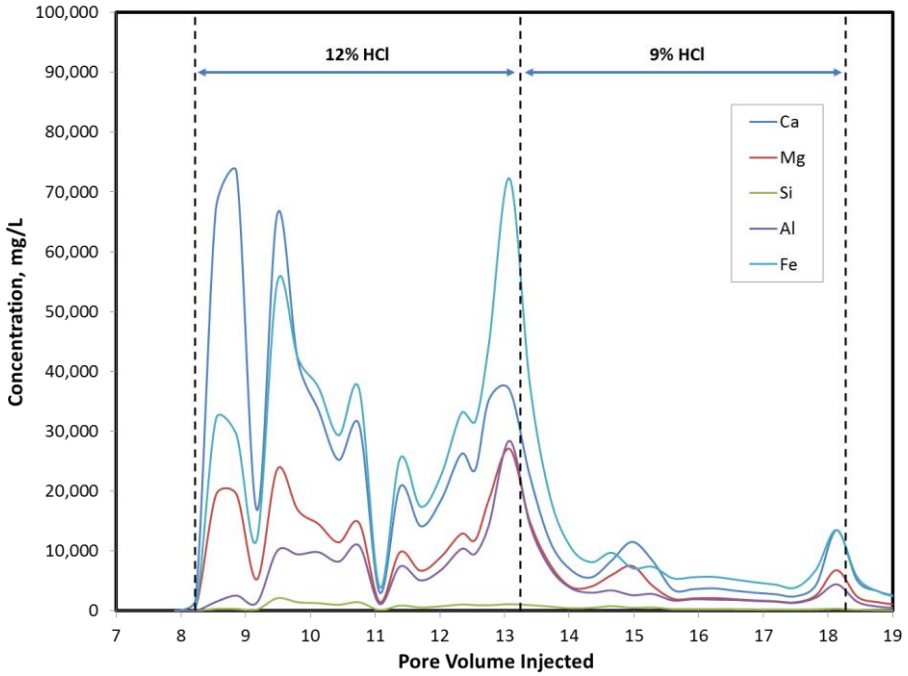

Figure 4.4 - ICP analysis for 0% HF experiment with Bandera core.

The second experiment (**Fig. 4.5 to Fig. 4.8**) was performed using 5 pore volumes of 12 wt% HCl as a preflush fluid and 5 pore volumes of 9 wt% HCl + 0.5 wt% HF as main acid. Compared to the 0 wt% HF experiment a slightly higher permeability enhancement was achieved indicating that the 0.5 wt% HF was able to achieve extra permeability enhancement by dissolving part of the mineral content of the formation.

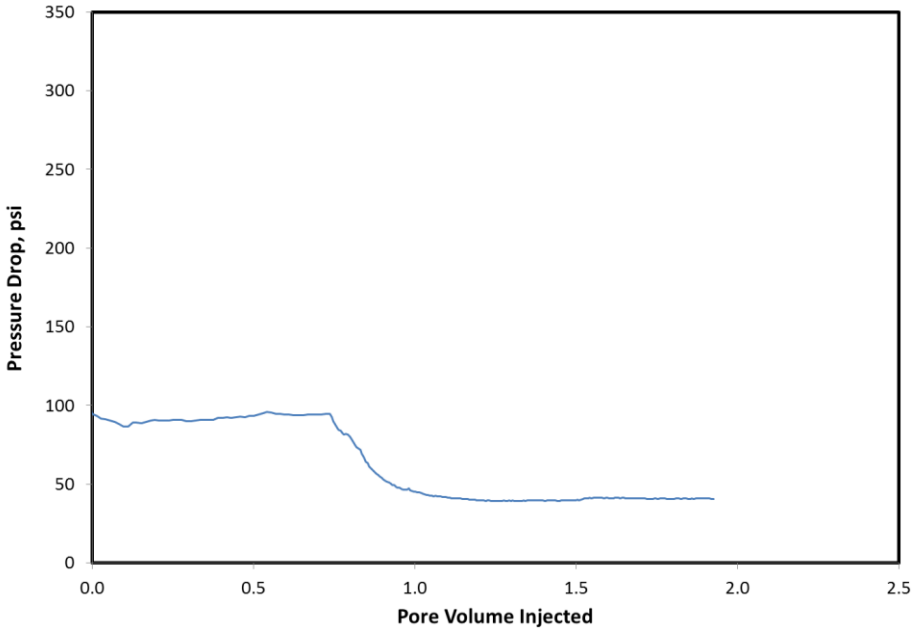

Figure 4.5 - Initial permeability for core Ba-09.

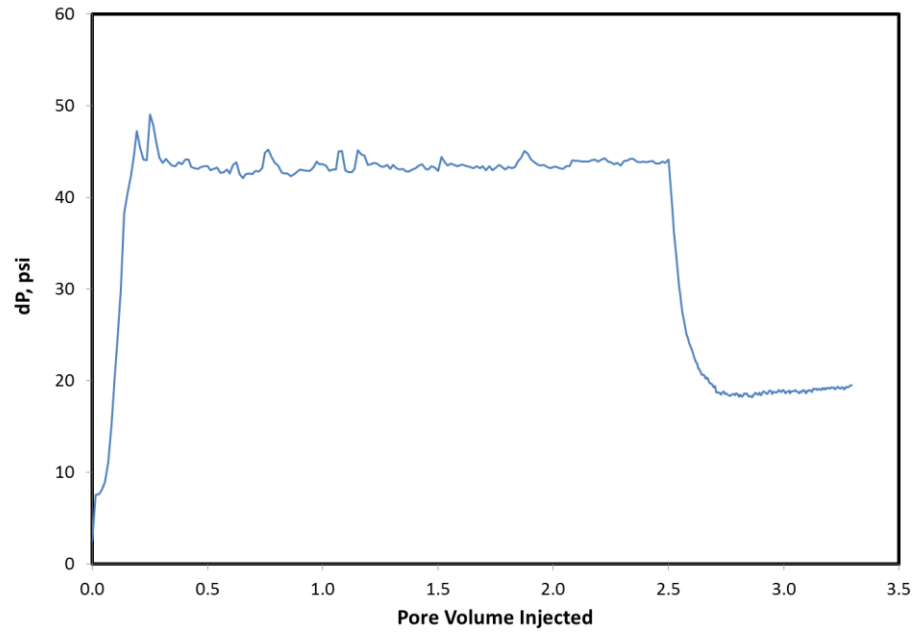

Figure 4.6 - Final permeability for core Ba-09.

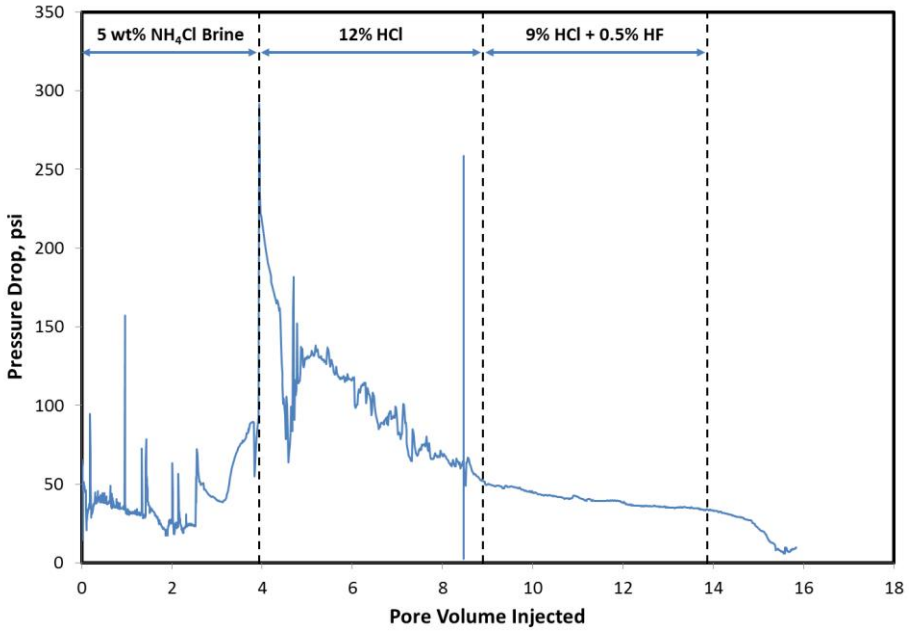

Figure 4.7 - Pressure drop curve during 0.5% HF experiment with Bandera core.

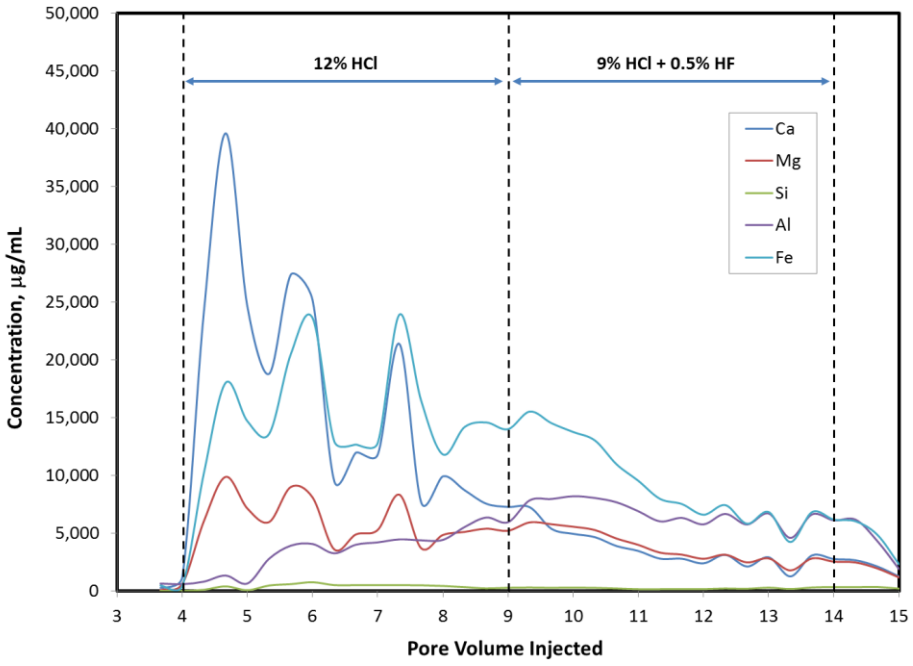

Figure 4.8 - ICP analysis for 0.5% HF experiment with Bandera core.

The third experiment (**Fig. 4.9 to Fig. 4.11**) was performed using 5 pore volumes of 12 wt% HCl as a preflush fluid and 5 pore volumes of 9 wt% HCl + 1 wt% HF as main acid. By increasing the HF concentration in the mud acid to 1%, mineral dissolution was achieved enhancing the permeability by three folds which is the best result in all Bandera experiments.

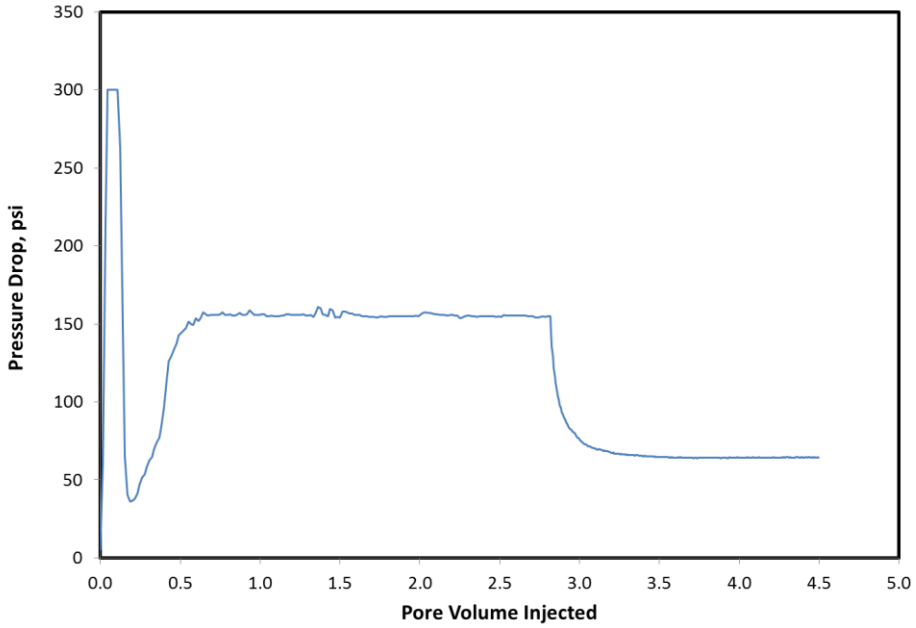

Figure 4.9 - Initial permeability for core Ba-07.

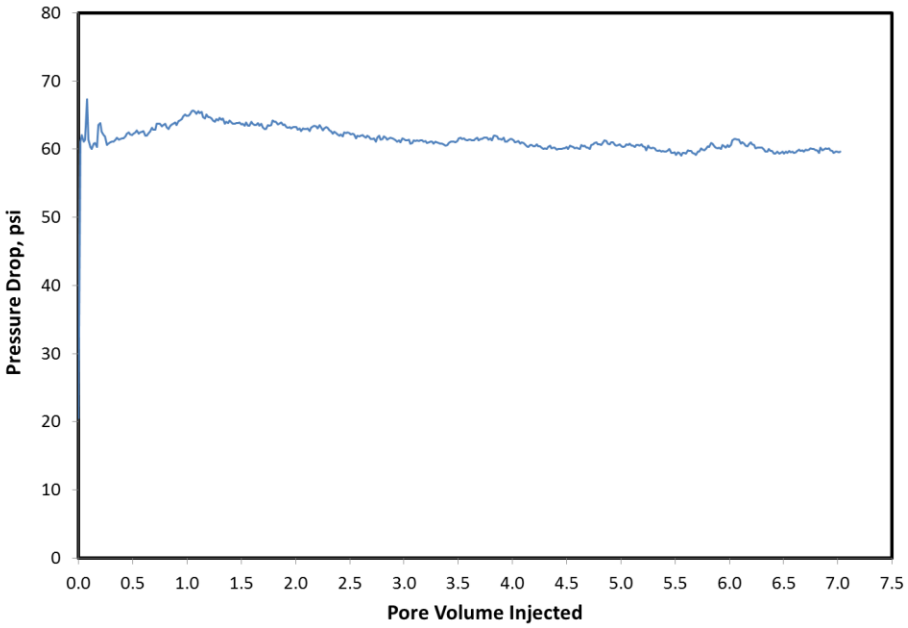

Figure 4.10 - Final permeability for core Ba-07.

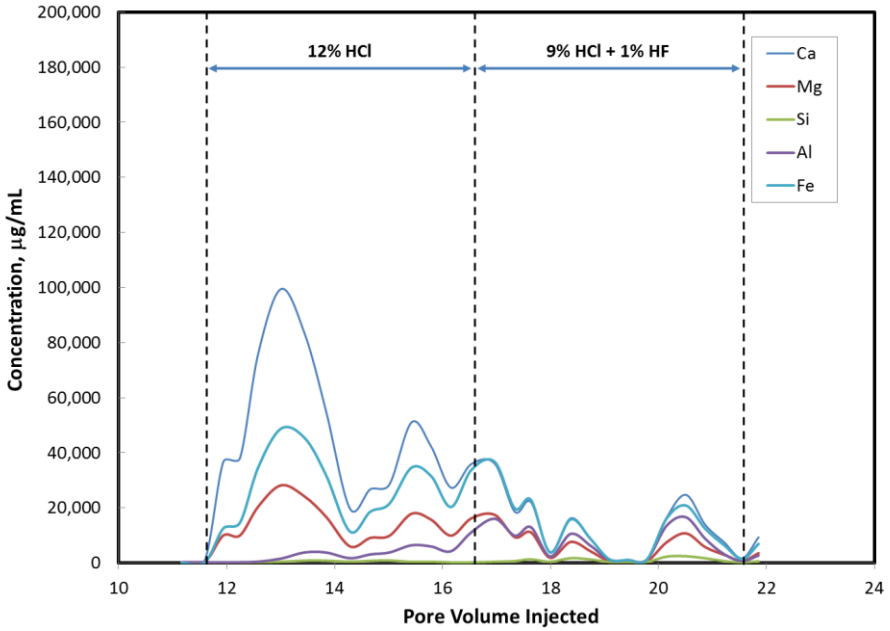

Figure 4.11 - ICP analysis for 1% HF experiment with Bandera core.

By increasing the HF concentration further to 1.5 wt% (**Fig. 4.12 to Fig. 4.15**), the permeability enhancement achieved was close to that of the experiment done by 0.5% HF and less than the enhancement achieved by the 1% HF mud acid. This is due to the occurrence of the secondary and tertiary reaction which is indicated by the low silicon to aluminum ratio (**Fig. 4.15**).

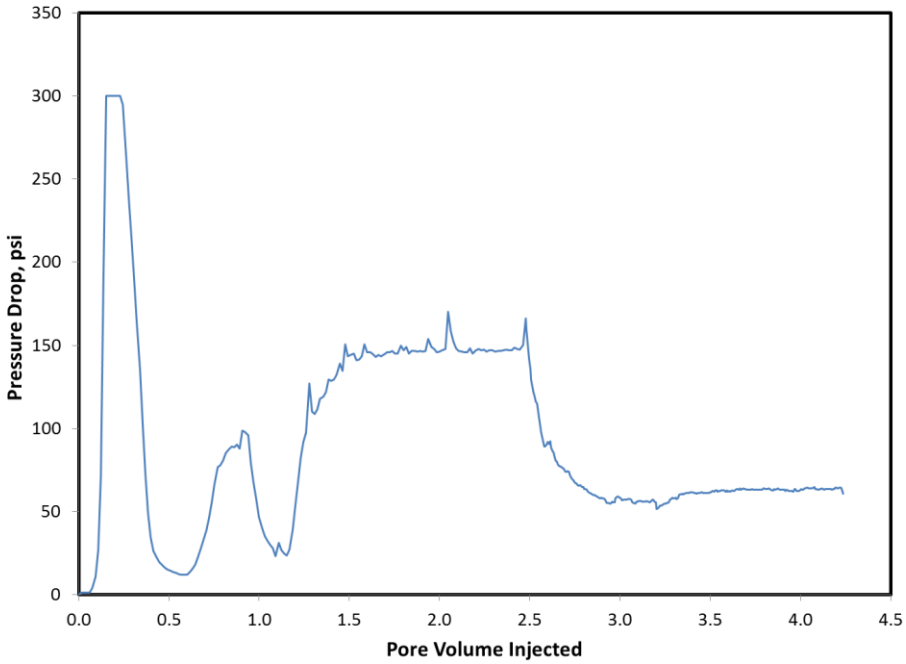

Figure 4.12 - Initial permeability for core Ba-08.

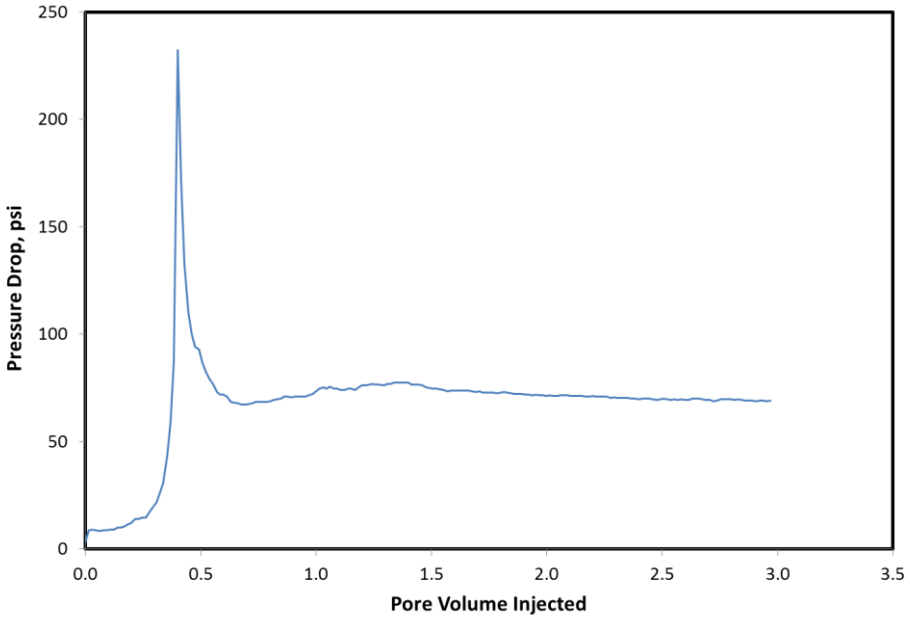

Figure 4.13 - Final permeability for core Ba-08.

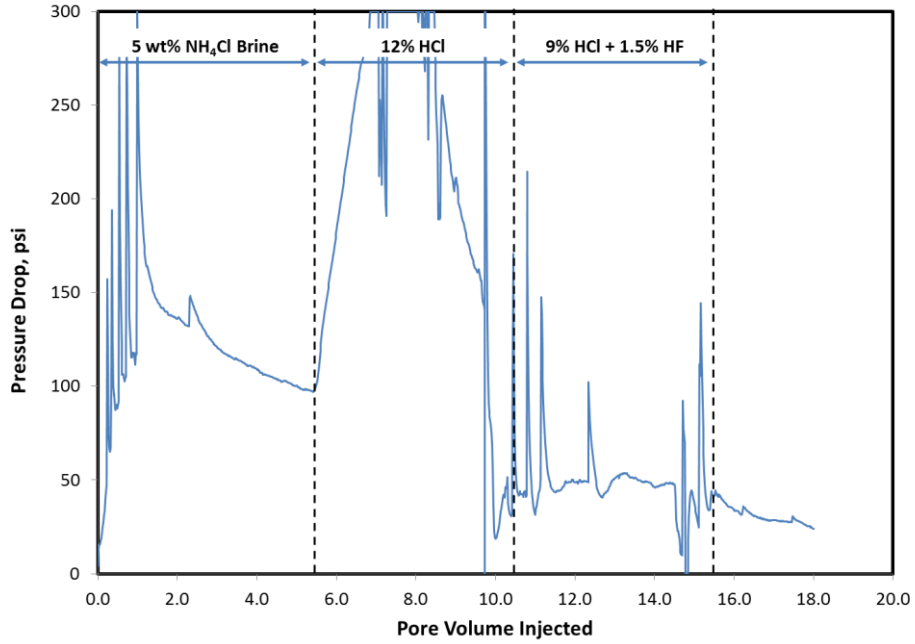

Figure 4.14 - Pressure drop curve during 1.5% HF experiment with Bandera core.

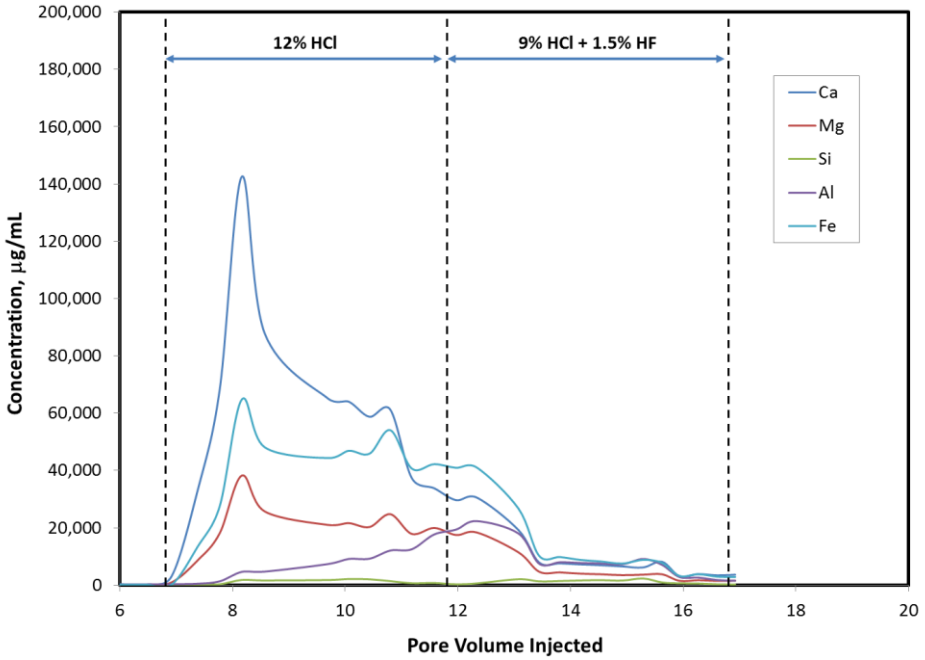

Figure 4.15 - ICP analysis for 1.5% HF experiment with Bandera core.

For the experiments done with even higher HF concentrations (2.5 and 3%) the results were even worse than when using just HCl which is due to the damage caused by the secondary and tertiary reactions (**Fig. 4.16 to Fig. 4.23**).

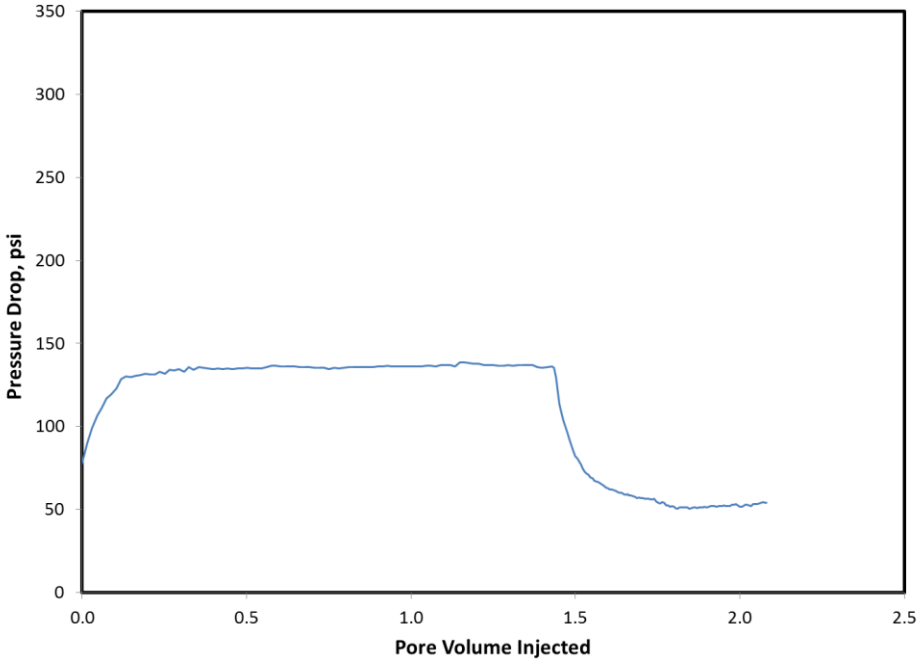

Figure 4.16 - Initial permeability for core Ba-04.

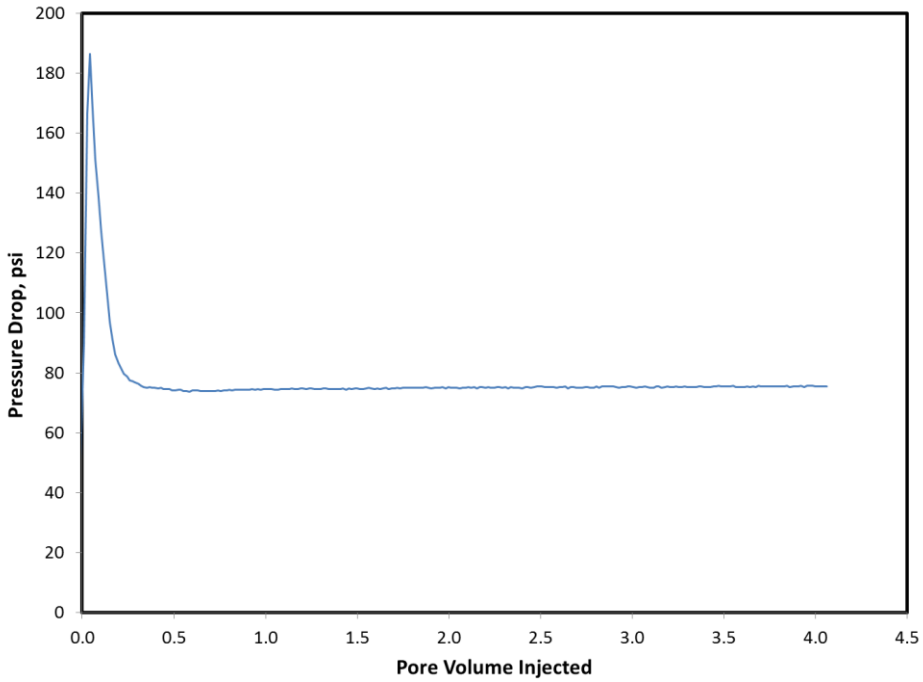

Figure 4.17 - Final permeability for core Ba-04.

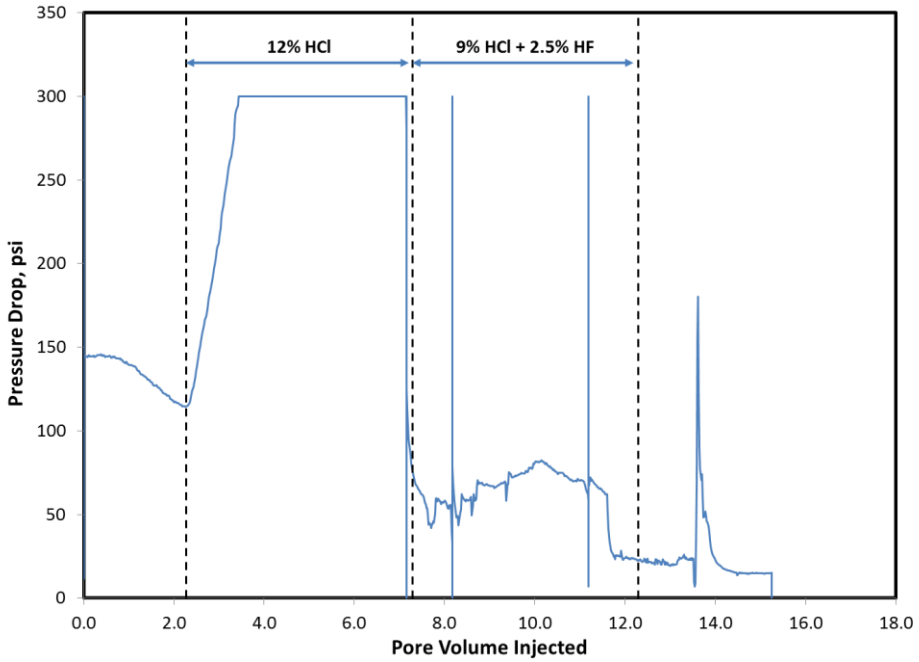

Figure 4.18 - Pressure drop curve during 2.5% HF experiment with Bandera core.

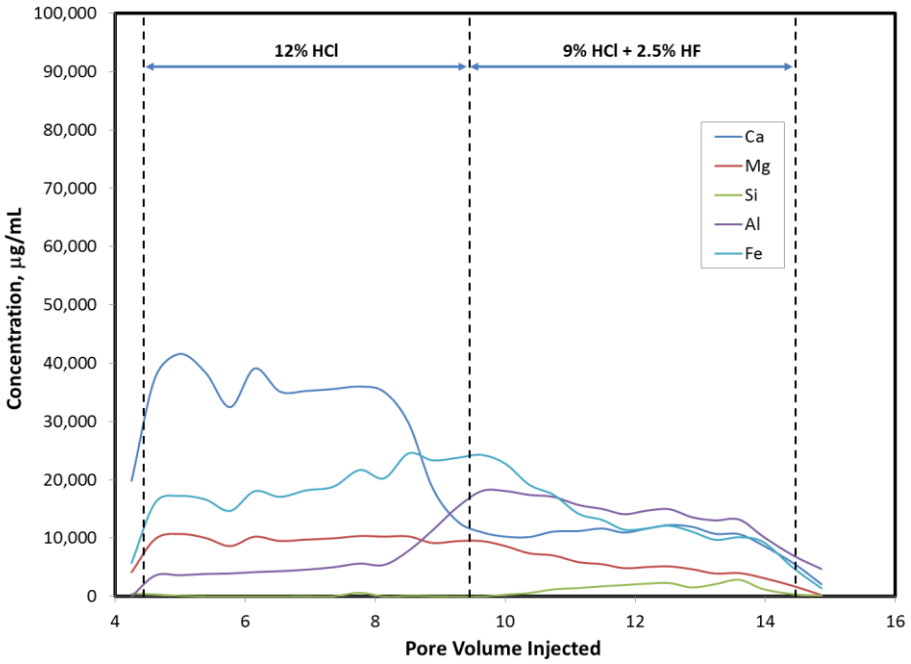

Figure 4.19 - ICP analysis for 2.5% HF experiment with Bandera core.

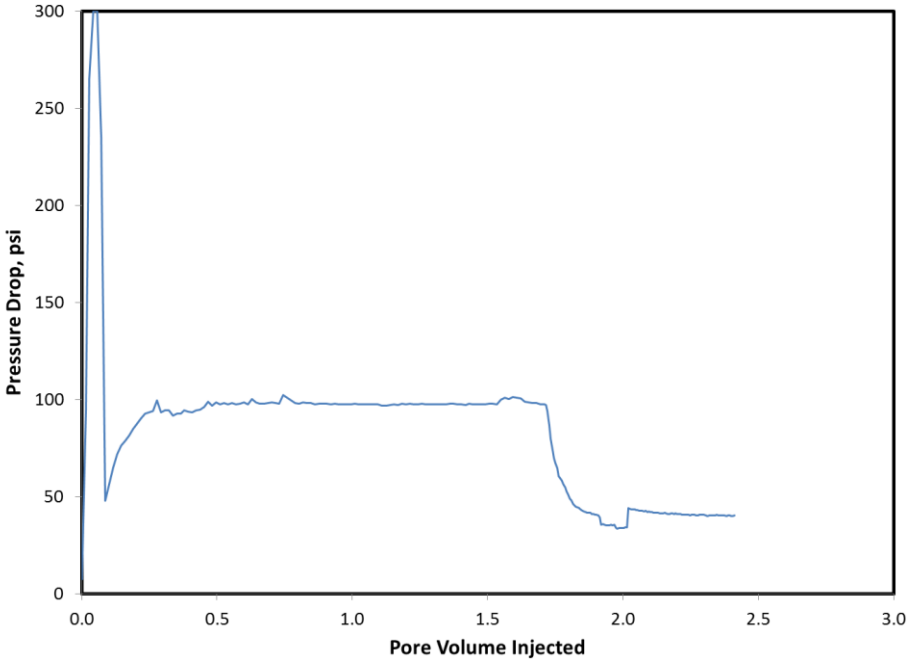

Figure 4.20 - Initial permeability for core Ba-05.

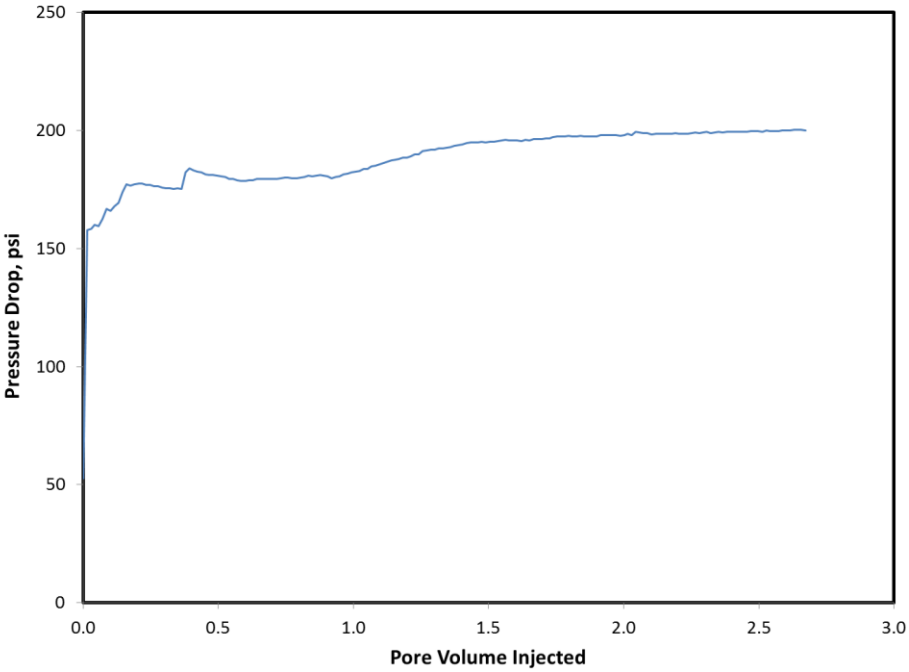

Figure 4.21 - Final permeability for core Ba-05.

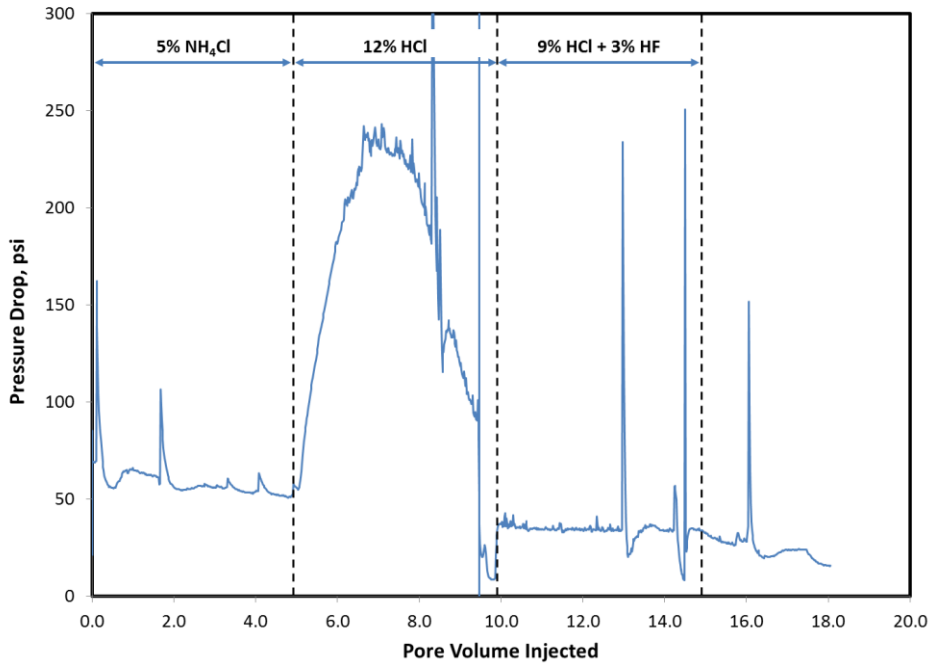

Figure 4.22 - Pressure drop curve during 3% HF experiment with Bandera core.

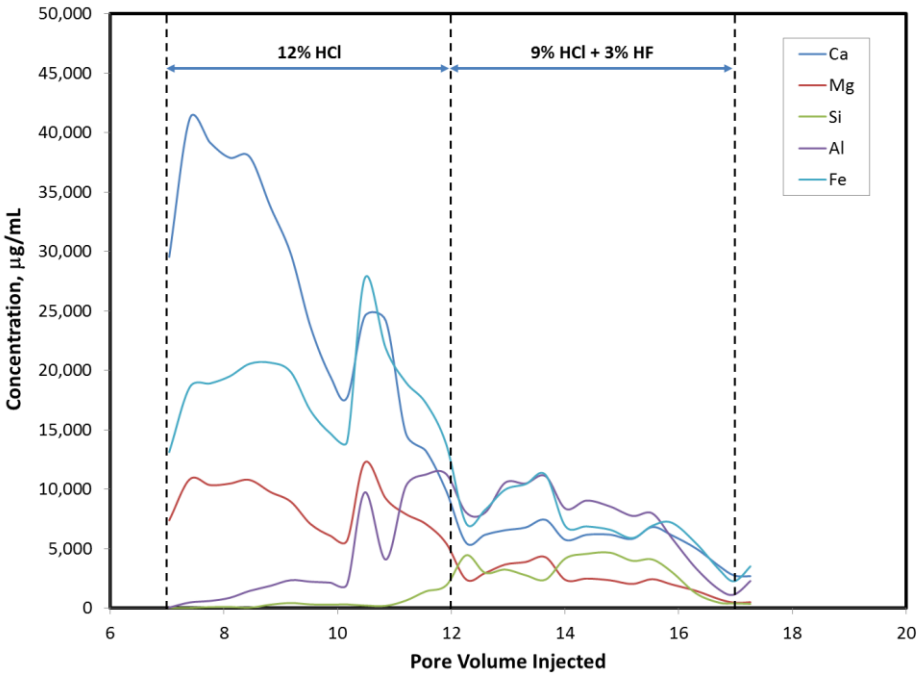

Figure 4.23 - ICP analysis for 3% HF experiment with Bandera core.

Fig. 4.24 represents a summary of all the experiments done on Bandera experiments. By fitting a trend between the points and equating the first derivative to zero, the optimum HF concentration can be identified to be 1.06 wt% as shown below.

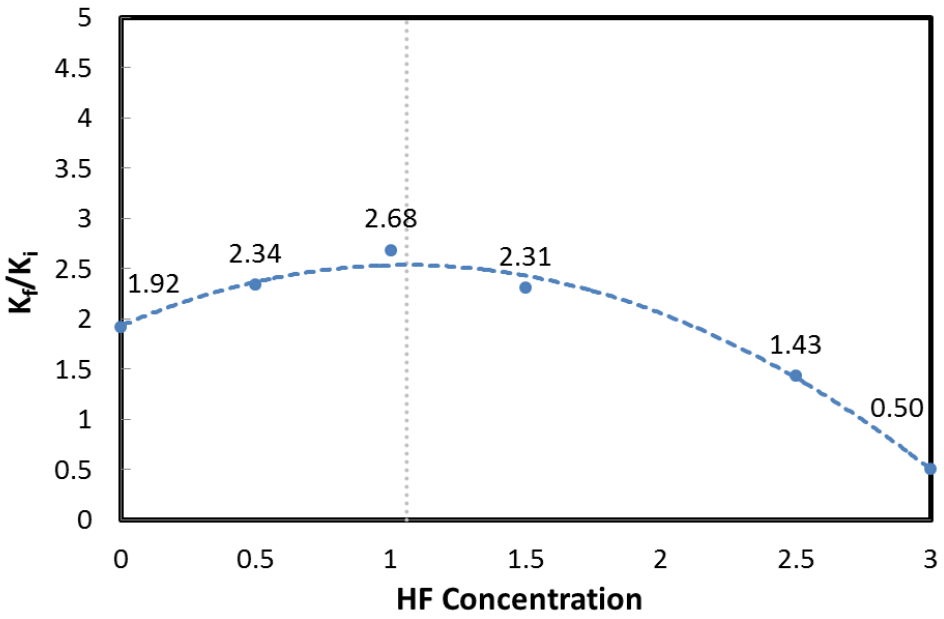

Figure 4.24 - Summary of Bandera sandstone experiments.

$$K_f/K_i = -0.5408\ HF^2 + 1.1443\ HF + 1.9302$$

$$\frac{d\ K_f/K_i}{d\ HF} = -1.0816\ HF + 1.1443$$

For $\frac{d\ K_f/K_i}{d\ HF} = 0$ then $1.0816\ HF = 1.1443$

$$\text{Optimum HF} = \frac{1.1443}{1.0816} = 1.058$$

Grey Berea Sandstone Experiments

The Grey Berea sandstone cores were tested to identify the optimum HF concentration; four experiments were done using concentrations of 1, 1.5, 2, and 2.5 wt%. **Table 4.3** has a list of all experiments done using Grey Berea sandstone experiments.

Table 4.3 - Grey Berea sandstone experiments summary.

Core ID	HF Concentration, wt%	Initial Permeability, md	Final Permeability, md	Kf/Ki
GB-06	1	61.44	61.02	0.993
GB-04	1.5	48.51	66.02	1.361
GB-02	2	43.03	51.31	1.192
GB-05	3	53.56	59.32	1.108

The first experiment was done using 1 wt% HF. five pore volumes of 12 wt% HCl was injected in the core followed by 5 pore volumes of 9 wt% of HCl + 1 wt% of HF as a main acid. As seen by comparing the initial and final permeability (**Fig. 4.25 and Fig. 4.26**) almost no change in the permeability was achieved. From the ICP analysis (**Fig. 4.28**) it can be seen that during the first three pore volumes, the high iron and medium aluminum content in the core effluent sample that is a result of dissolving the chlorite leaving an amorphous silica rich residue that damages the formation. Also during the same interval, calcium and magnesium were recorded and that is due to the dissolution of the 3% carbonate content. After injection of the main acid both silicon and aluminum were recorded in the effluent sample indicating the dissolution of the mineral content due to the injection of the mud acid. As a result of both carbonate and mineral dissolution from one side and the damage caused by HCl injection in a formation with

chlorite and illite content, both effects cancelled each other leaving the permeability unaltered.

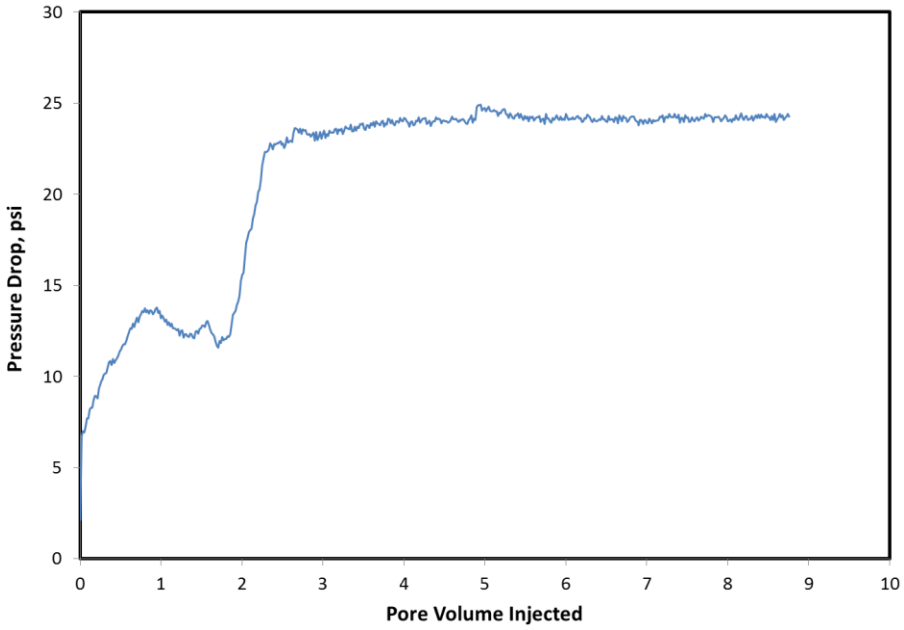

Figure 4.25 - Initial permeability for core GB-06.

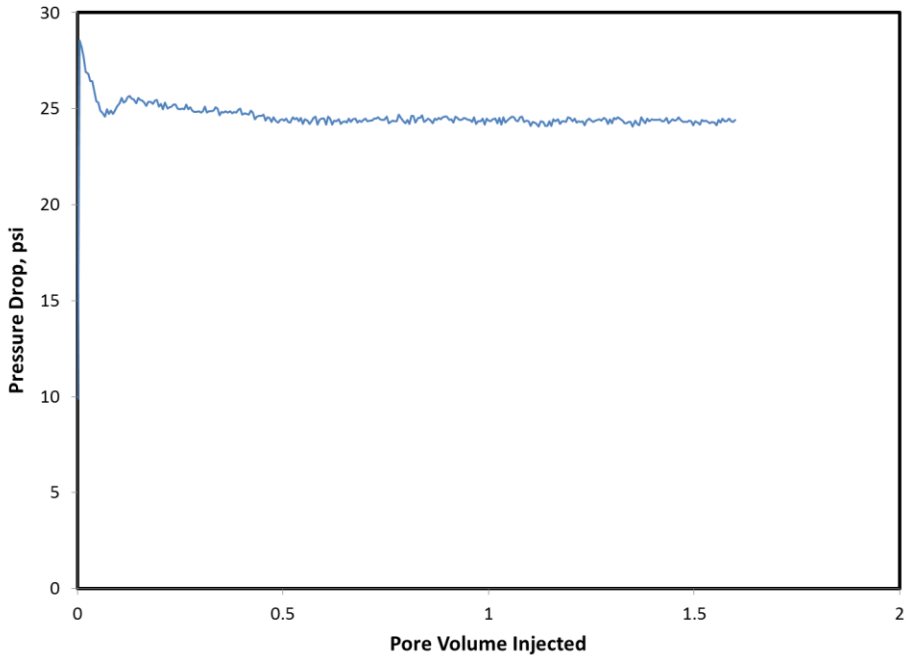

Figure 4.26 - Final permeability for core GB-06.

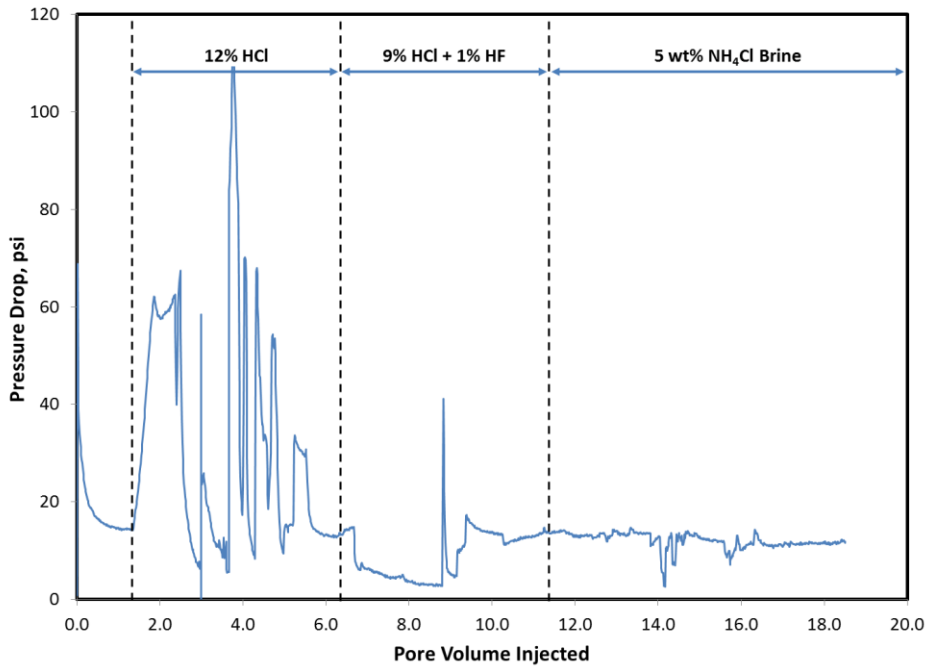

Figure 4.27 - Pressure drop curve during 1% HF experiment with Grey Berea core.

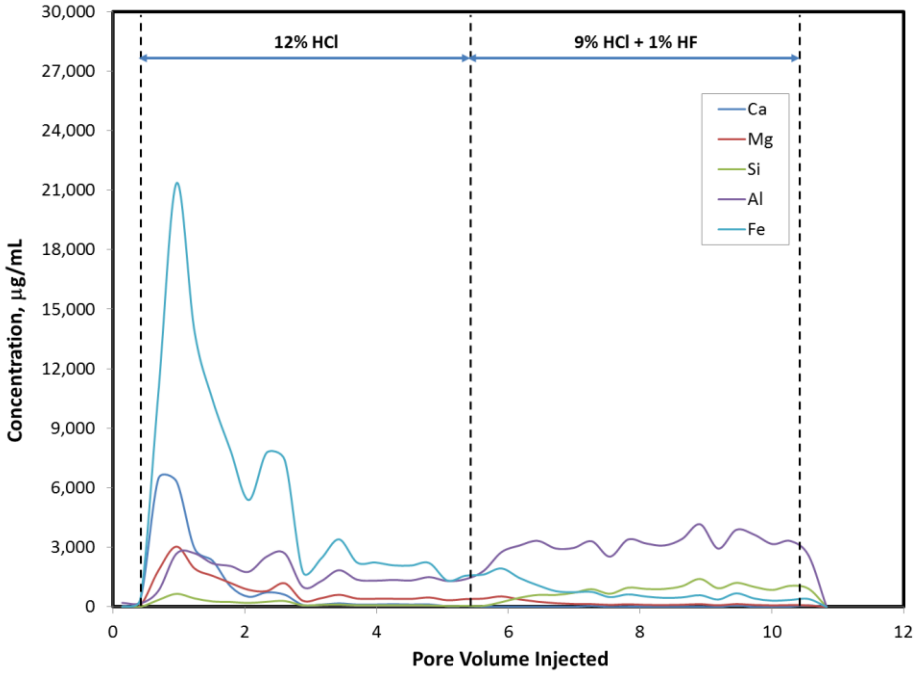

Figure 4.28 - ICP analysis for 1% HF experiment with Grey Berea core.

The second experiment (**Fig. 4.29 to Fig. 4.32**) was performed using 5 pore volumes of 12 wt% HCl as a preflush fluid and 5 pore volumes of 9 wt% HCl + 1.5 wt% HF as main acid. Compared to the 1% HF experiment a higher content of aluminum and silicon was noticed during the main acid injection period which was due to the dissolving of more minerals resulting in enhancement of the permeability of the core.

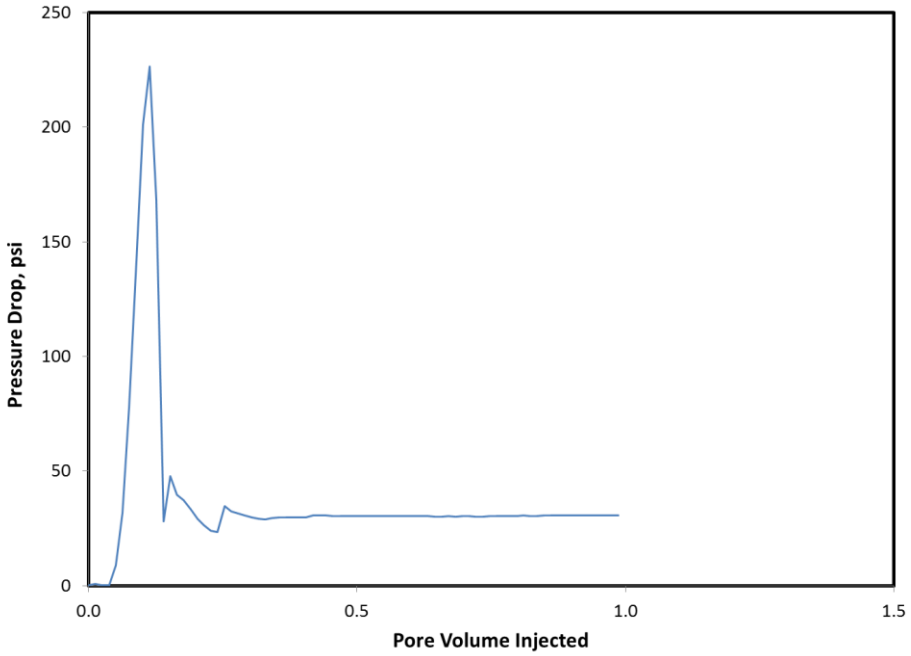

Figure 4.29 - Initial permeability for core GB-04.

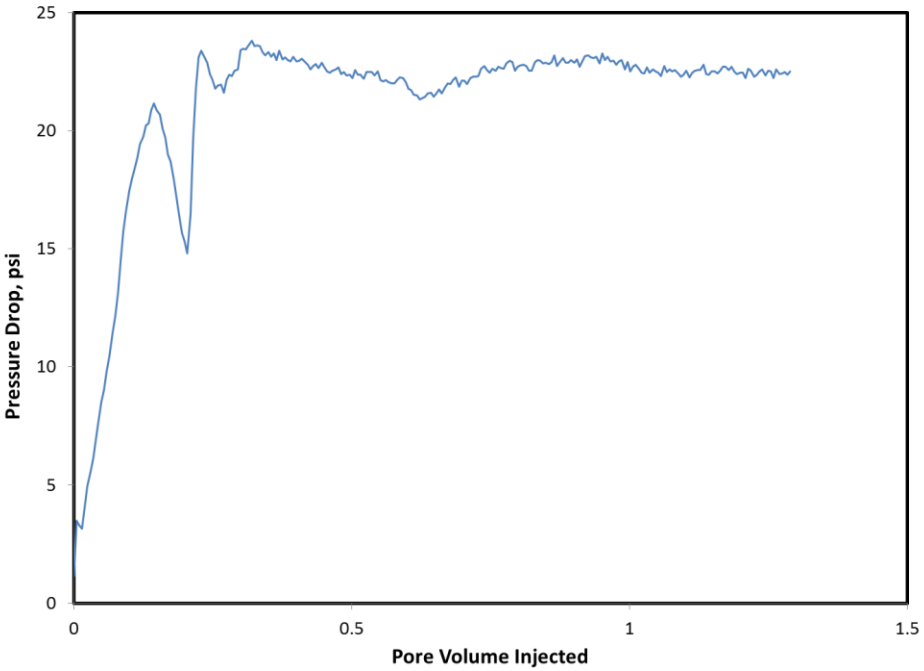

Figure 4.30 - Final permeability for core GB-04.

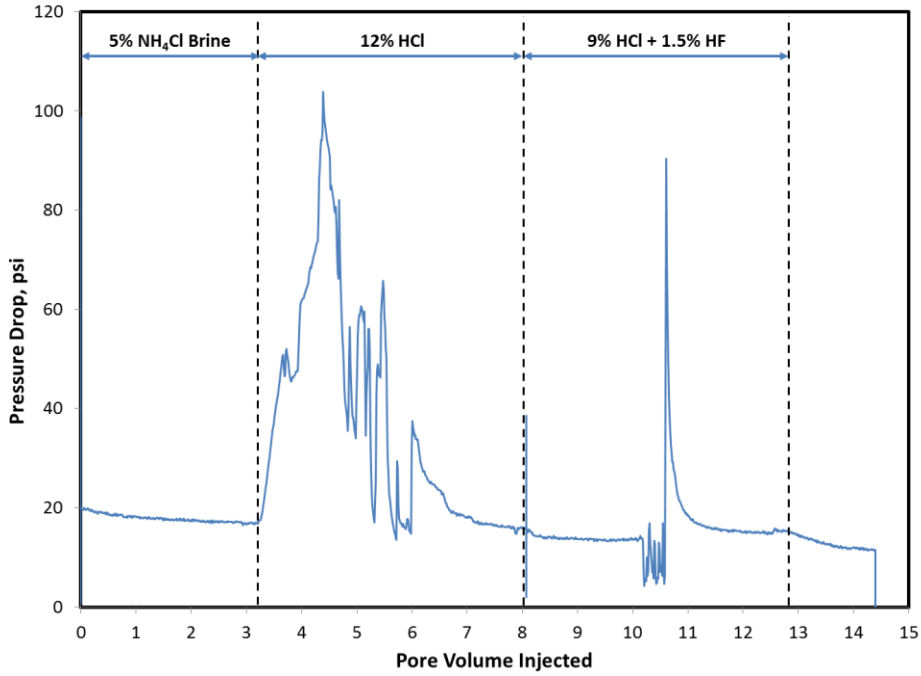

Figure 4.31 - Pressure drop curve during 1.5% HF experiment with Grey Berea core.

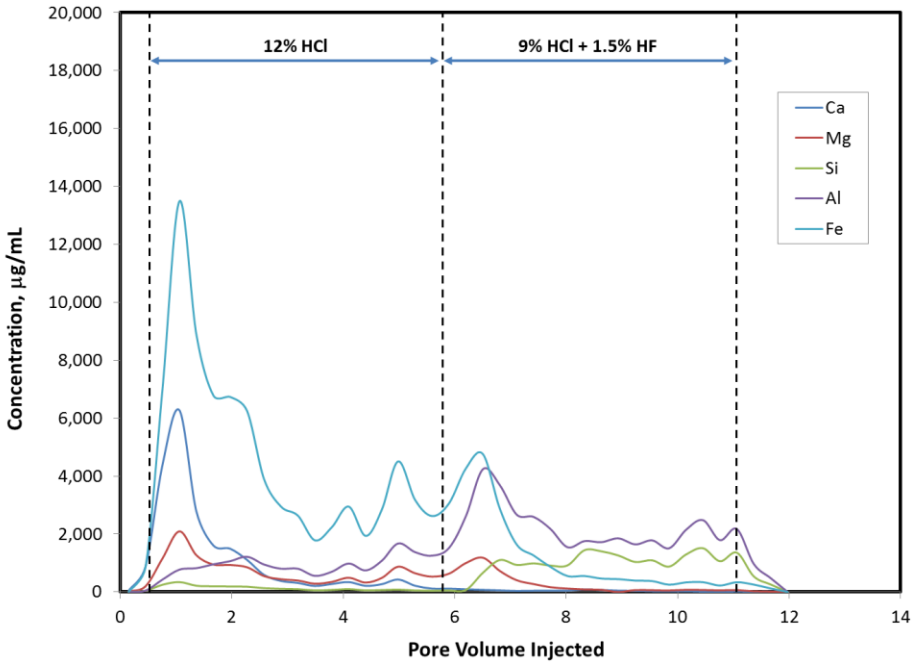

Figure 4.32 - ICP analysis for 1.5% HF experiment with Grey Berea core.

The third experiment (**Fig. 4.33 to Fig. 4.36**) was performed using 5 pore volumes of 12 wt% HCl as a preflush fluid and 5 pore volumes of 9 wt% HCl + 2 wt% HF as main acid. Compared to the 1.5% HF experiment, the permeability enhancement achieved by this experiment was lower than that achieved by injecting 1.5 wt% HF indicating that damage occurred due to the secondary and tertiary reaction as could be seen in the ICP analysis (**Fig. 4.36**).

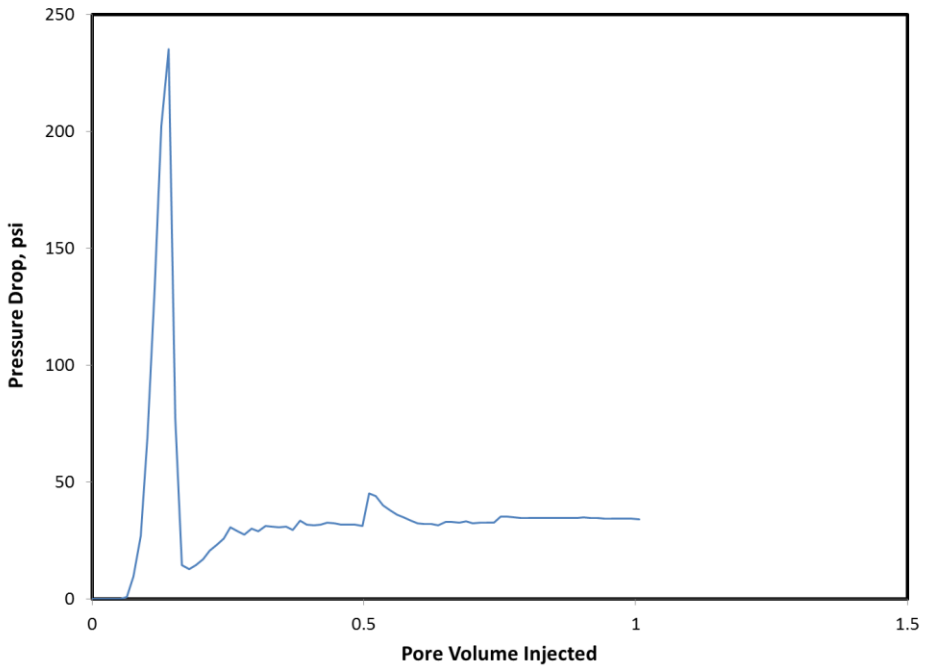

Figure 4.33 - Initial permeability for core GB-02.

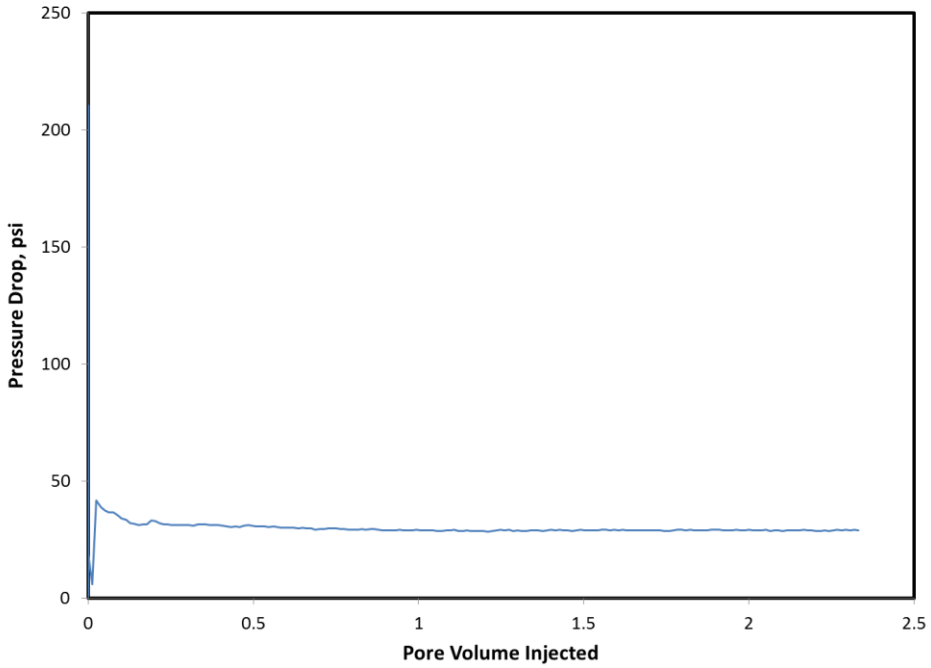

Figure 4.34 - Final permeability for core GB-02.

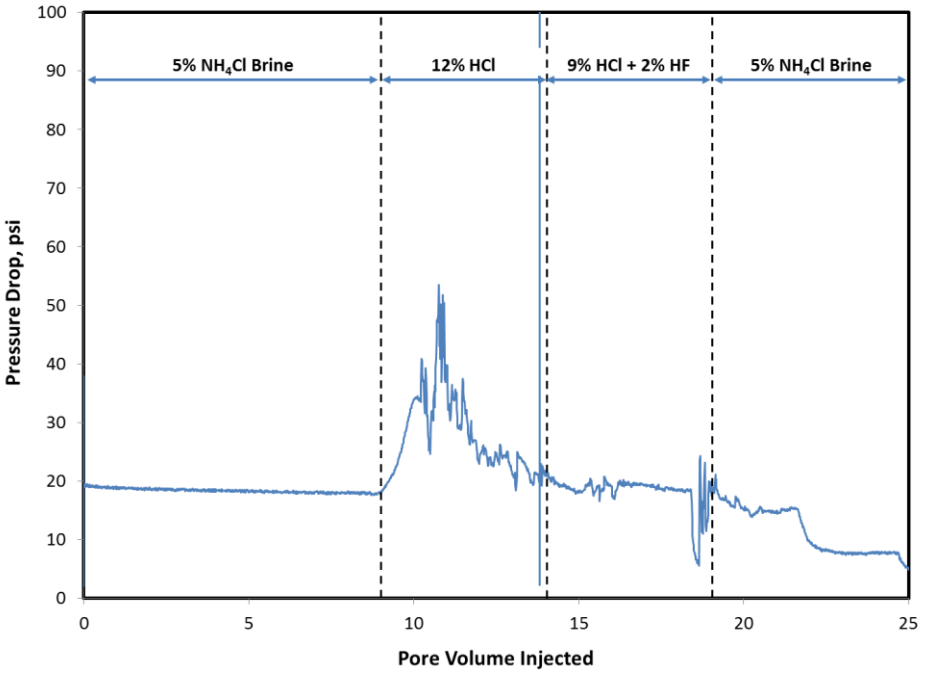

Figure 4.35 - Pressure drop curve during 2% HF experiment with Grey Berea core.

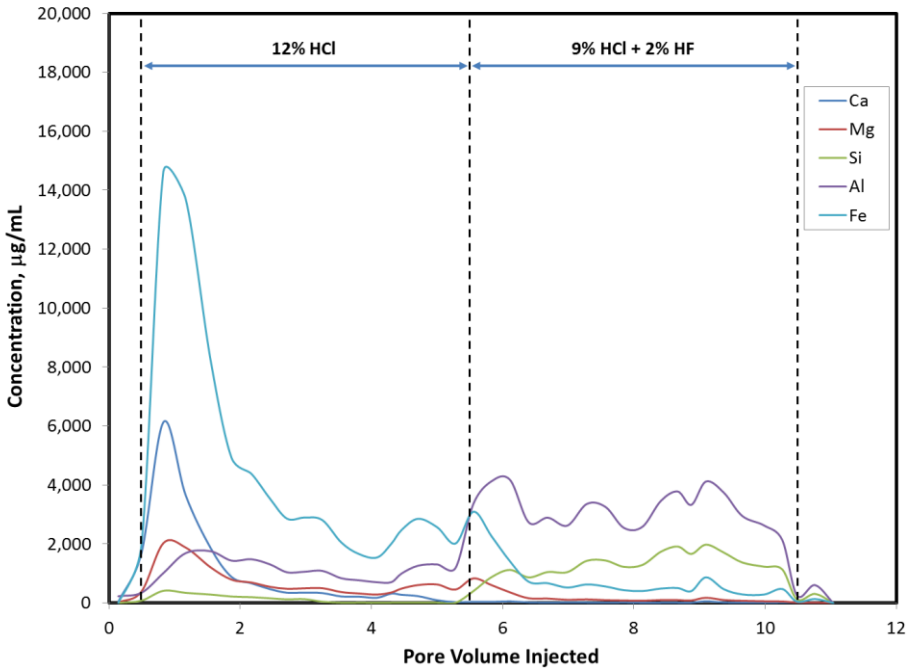

Figure 4.36 - ICP analysis for 2% HF experiment with Grey Berea core.

Finally, by increasing the HF concentration further to 2.5 wt% (**Fig. 4.37 and Fig. 4.40**) more damage occured to the core resulting in a lower permeability ratio than that achieved by 2 or 1.5 wt%.

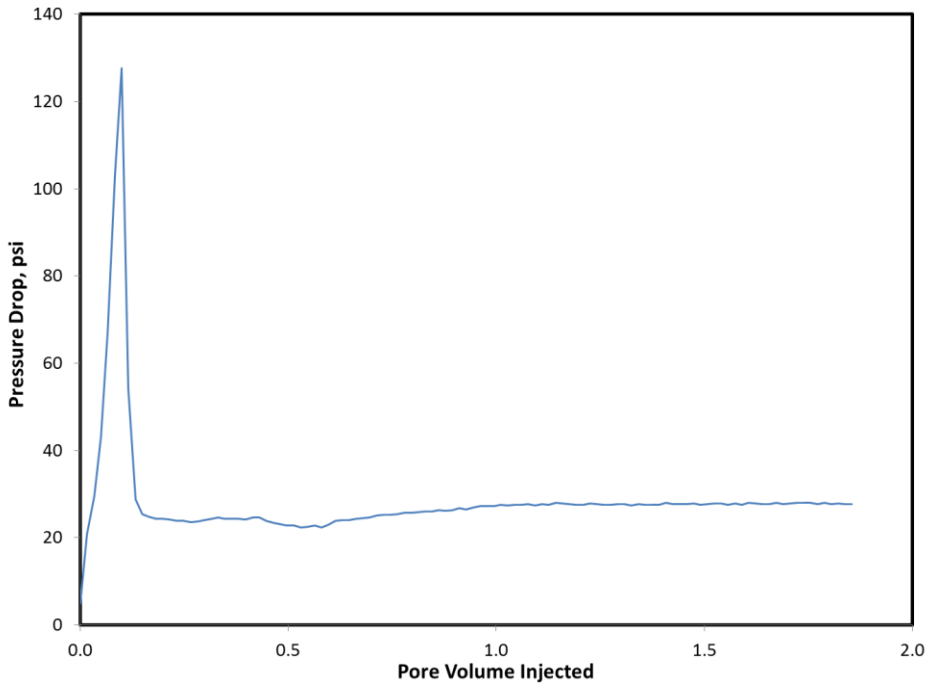

Figure 4.37 - Initial permeability for core GB-05.

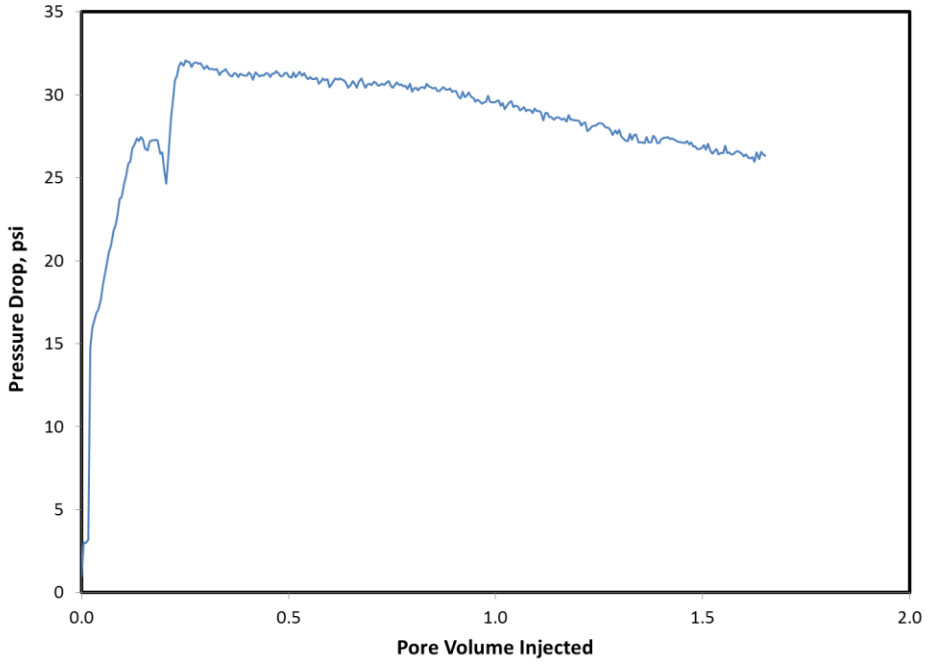

Figure 4.38 - Final permeability for core GB-05.

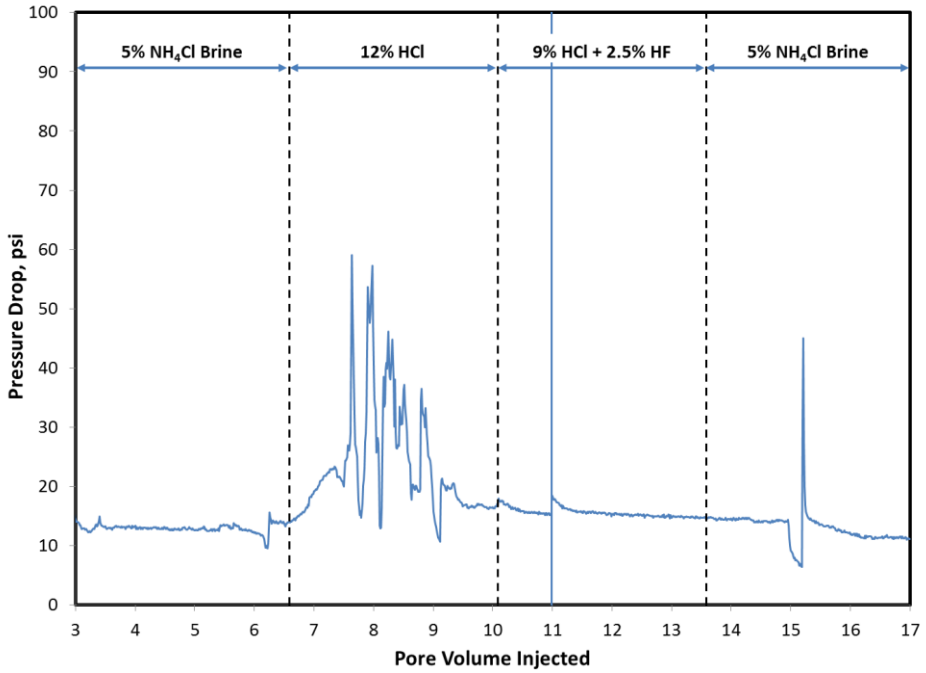

Figure 4.39 - Pressure drop curve during 2.5% HF experiment with Grey Berea core.

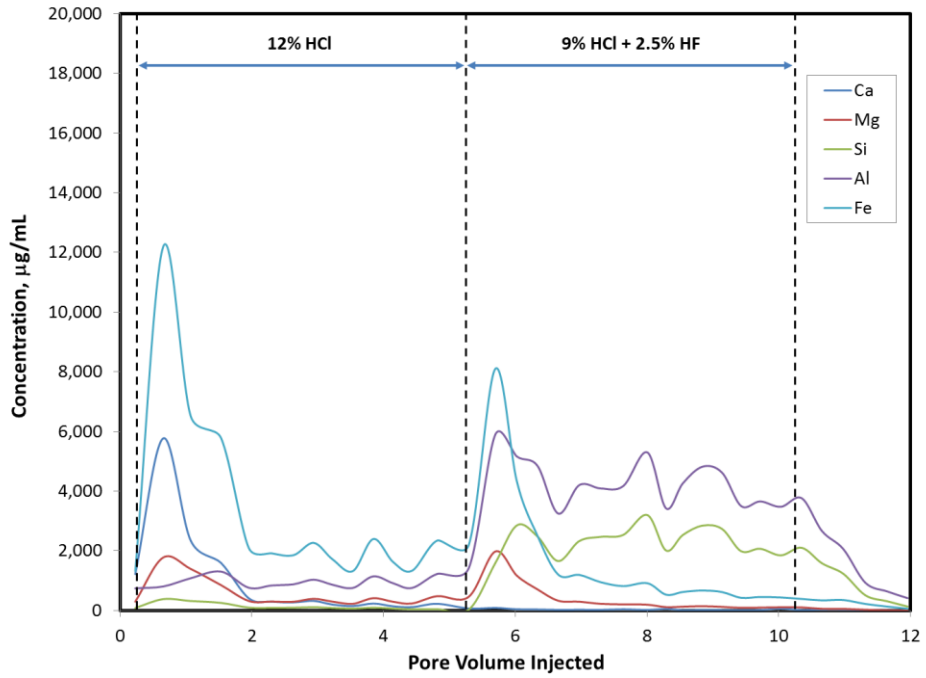

Figure 4.40 - ICP analysis for 2.5% HF experiment with Grey Berea core.

Fig. 4.41 represents a summary of all the experiments done on Grey Berea experiments. By fitting a trend between the points and equating the first derivative to zero, the optimum HF concentration can be identified to be 1.79 wt% as shown below.

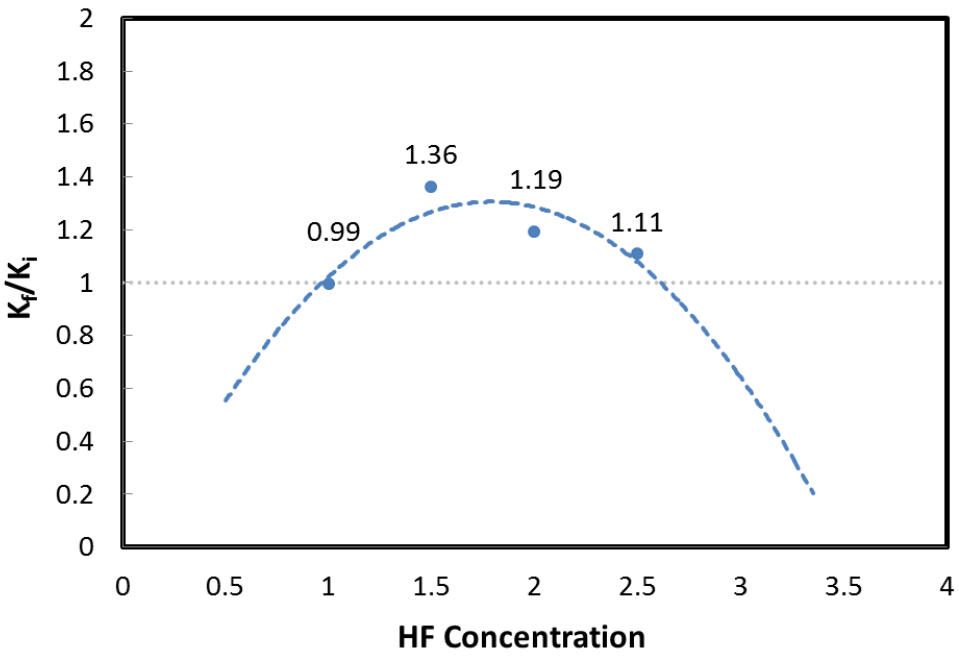

Figure 4.41 - Summary of Grey Berea sandstone experiments.

$$\frac{K_f}{K_i} = -0.4527\ HF^2 + 1.6195\ HF - 0.1426$$

$$\frac{d\ K_f/K_i}{d\ HF} = -0.9054\ HF + 1.6195$$

For $\frac{d\ K_f/K_i}{d\ HF} = 0$ then $0.9054\ HF = 1.6195$

$$\text{Optimum HF} = \frac{1.6195}{0.9054} = 1.789$$

CHAPTER V

ACIDIZING SOFTWARE

Advisory System

Where a high HCl solubility exists (20% or more) HF acid should not be used. Damage can generally be loosened by dissolving the HCl acid soluble compounds (McLeod et al. 1983). This represents the first screening criteria in the decision tree. In general the reservoirs with 20% of HCl soluble components (usually carbonates) are treated using the same decision criteria used for the carbonate reservoirs.

Table 5.1 - Stability limits of clays (Coulter and Jennings 1999).

Clay	Stability Limit
Kaolinite	200°F
Smectite	150°F
Illite	150°F
Chlorite	125°F

Several studies discussed the stability of clays in HCl, and all previous work has shown that all clays tend to become unstable in HCl. **Table 5.1** summarizes the limits for the stability of different clays as reported by Coulter and Jennings (1999). The temperatures reported by Coulter and Jennings were chosen as they are conservative compared to the numbers reported in literature (Shuchart and Gdanski 1996; Simon and

Anderson 1990). On the other hand, feldspars were reported to be stable at temperatures of up to 350°F (Gdanski 1998).

The first module of the decision tree (**Fig. 5.1**) aims to determine whether HCl can be used in the formulation of mud acid or it should be replaced with a weaker organic acid. The theory behind the decision comes from the fact that clays become unstable in HCl at the high temperatures. Starting with the kaolinite which is the most stable clay (Gdanski 1998). Coulter and Jennings reported that the kaolinite becomes unstable in HCl at a temperature of 200°F (Coulter and Jennings 1999). This means that at temperatures that are higher than 200°F, it is preferred to use organic acid regardless of the composition.

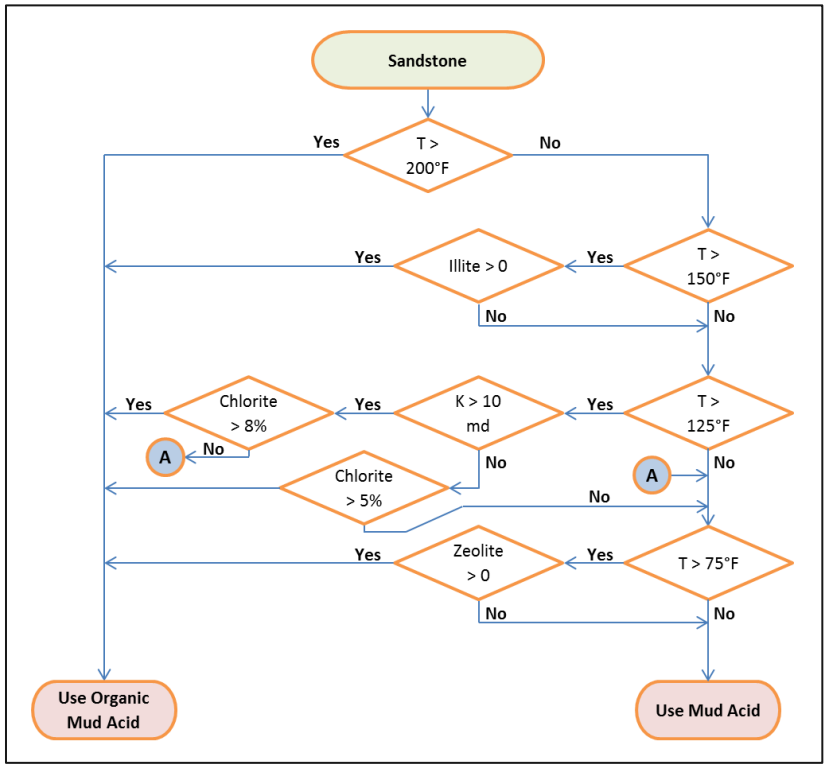

Figure 5.1 - The first module of the decision tree.

After that comes the Illite, which becomes unstable at temperatures higher than 150°F. So in the presence of illite, it is better if organic mud acid is used than regular mud acid. The chlorite was reported to become unstable in HCl at temperatures above 125°F. Mcleod suggested using a cutoff value of 8% for medium (10 to 100 md) and high permeability (>100 md) reservoirs, while he used a cutoff value of 5% for the low permeability reservoirs (<10 md). Finally, the zeolites are inherently more unstable because of their open structure. The zeolites will decompose and/or gelatinize in HCl at temperatures above approximately 75°F (Coulter and Jennings 1999). By going through these steps a decision is made between using mud acid or organic mud acid. This decision is based on the temperature, permeability, and mineral composition.

Next in the decision tree is to determine the percentage of both the HF acid and the HCl (or Formic/Acetic in organic mud acid). The curves previously determined in Chapter II were used to calculate the HF concentration in the software. To include this part in the graphical interface each curve had to be represented by an equation.

1% HF: $Y = 0.1679x^2 - 0.2686x + 0.1406$

1.5% HF: $Y = 0.2243x^2 - 0.2938x + 0.1167$

2.5% HF: $Y = 0.3071x^2 - 0.3135x + 0.0794$

3% HF: $Y = 0.435x^2 - 0.3324x + 0.0609$, for x<30%, $Y = 0$ otherwise

4% HF: $Y = 0.8267x^2 - 0.3627x + 0.036$, for x<15%, $Y = 0$ otherwise

where:

X is the Feldspar Content in fraction

Y is the Clay Content in fraction

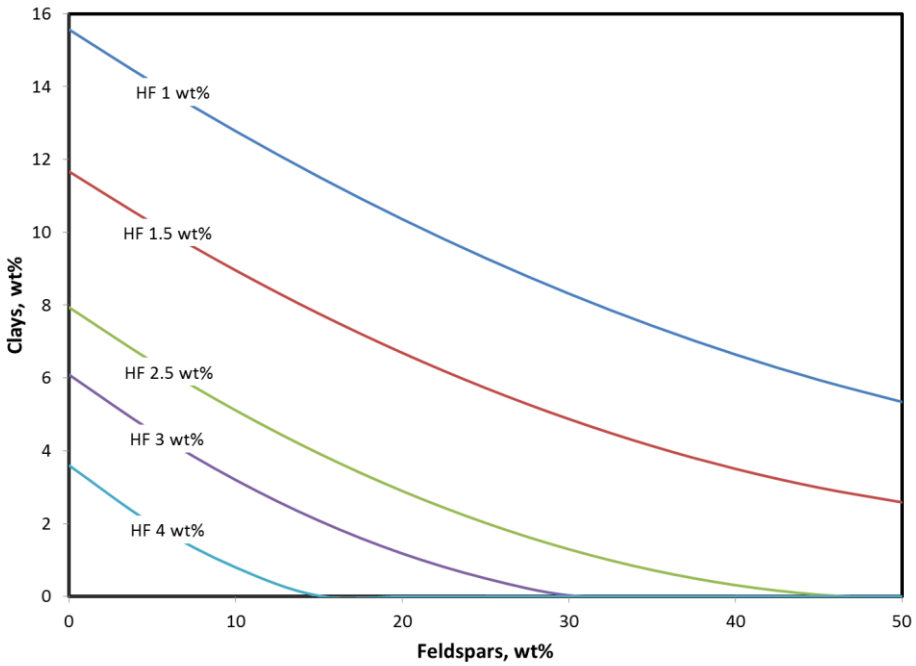

Figure 5.2 - The optimum HF concentration based on mineralogy.

The HCl concentration in the mud acid was found to be dependent on both the carbonate content of the rock and the designed HF concentration. Walsh et al. showed the relation between the HF concentration, calcite content, and the minimum required HCl concentration (Walsh et al. 1982). For the purpose of the design, the data was extracted from the figure and it was reconstructed so that the calcite content was represented on the "X" axis, the minimum HCl concentration was represented by the "Y" axis, and several curves were plotted so that each curve represented a different HF concentration. The reconstructed plot is shown in **Fig. 5.3**.

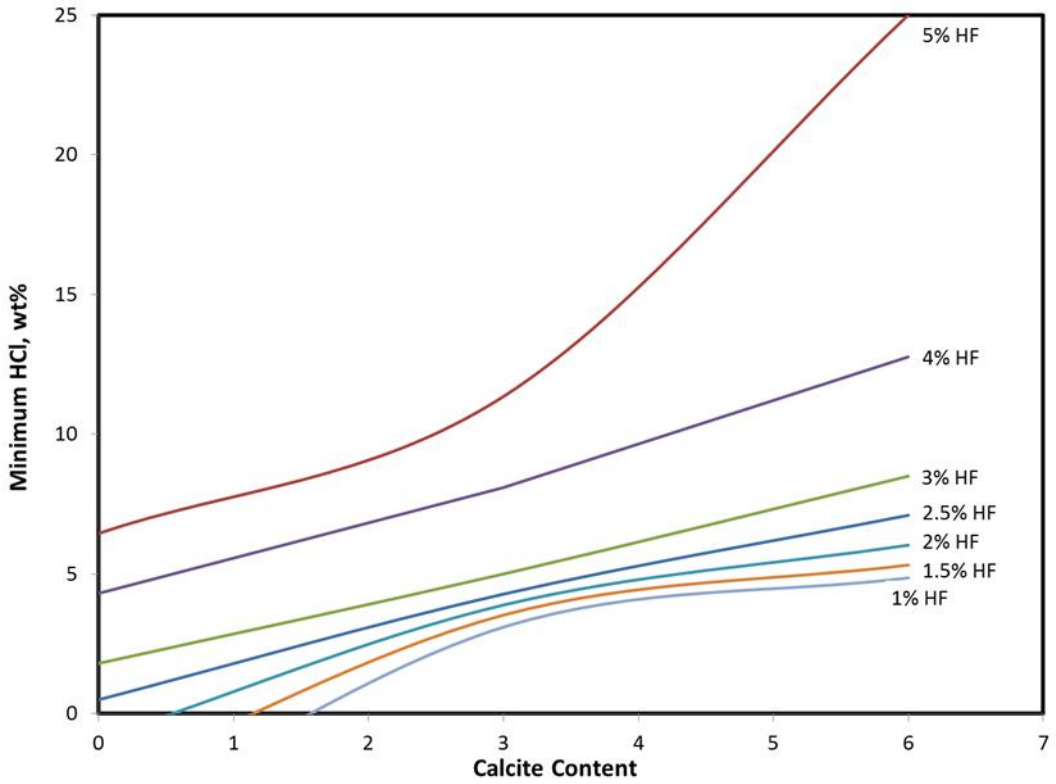

Figure 5.3 - Minimum required HCl based on calcite content and HF concentration.

The shown curves were used to determine the HCl concentration in the software. To include this part in the graphical interface, each curve had to be represented by the following equations:

1% HF: $Y = -5.2527 + 427.08x - 5860x^2 + 26369x^3$

1.5% HF: $Y = -4.1337 + 397.06x - 5586.1x^2 + 26293x^3$

2% HF: $Y = -0.9839 + 214.13x - 2083.9x^2 + 7904.4x^3$

2.5% HF: $Y = 0.5 + 142x - 533.33x^2$

3% HF: $Y = 1.8 + 101.67x - 166.67x^2$

4% HF: $Y = 4.3 + 112.17x + 483.33x^2$

5% HF: $Y = 6.45 + 17.5x + 4861.1x^2$

6% HF: $Y = 8.2 + 34.667x + 5755.6x^2$

where:

X is the HF concentration in wt%

Y is the HCl concentration in wt%

The curves (**Fig. 5.3**) determine the HCl concentration to be used in mud acid, but if the decision was made to use organic mud acid, an equivalent concentration of the organic acid (formic or acetic) is needed for the design. The equivalent concentration of organic acid is calculated by multiplying the previously determined concentration by a correction factor. **Fig. 5.4** represents a correction factor "CAcetic" and "CFormic" which when multiplied by the HCl concentration, will give the equivalent acetic and formic concentrations, respectively.

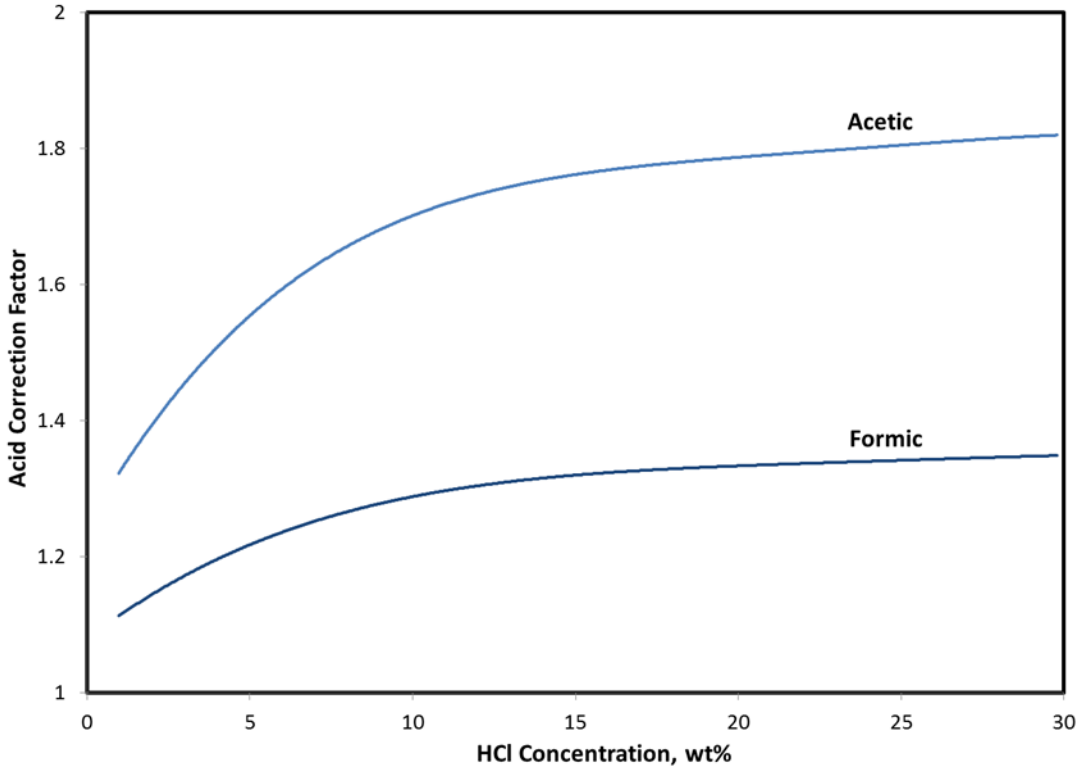

Figure 5.4 - Correction factor for organic acid concentration.

Graphical Interface

Running Acid Design

File Menu

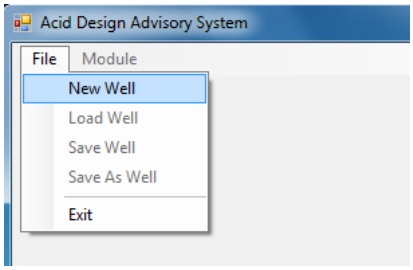

Figure 5.5 - File menu.

New Well

The "New Well" loads a form where you input the name of the company, field, and well. This information is used for keeping track of the different treatment reports produced by the software.

Load Well

The "Load Well" option will open a pop-up window for you to browse and select the previously saved wells to load.

Module Menu

The module menu lets you choose between wellbore cleanup module which designs treatments for the damage in the wellbore or matrix acidizing module which designs treatments for near wellbore damage.

Wellbore Cleanup

Click on the "Module" dropdown menu and select "Wellbore Cleanup".

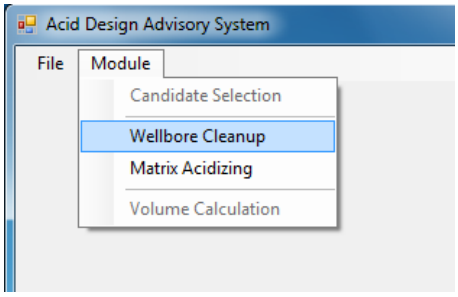

Figure 5.6 - Module menu.

A popup window will appear giving you the option to select the different types of wellbore damage that are present in the subject well (could be identified by the "Candidate Selection" module).

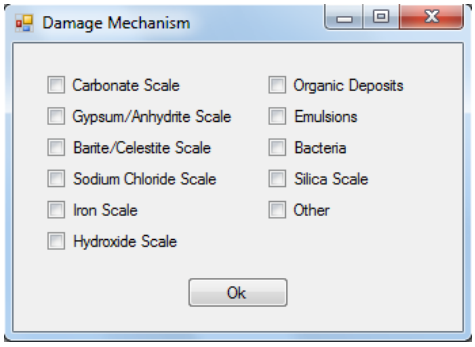

Figure 5.7 - Wellbore cleanup module.

Choose the type(s) of wellbore damage present in the well then click "Ok". A popup window will present the best treatment for the selected wellbore damaging mechanism(s).

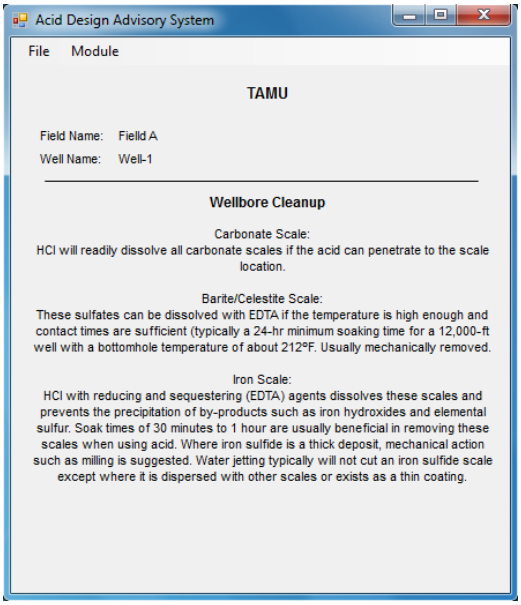

Figure 5.8 - Wellbore cleanup report.

Matrix Acidizing

The matrix acidizing module designs treatments for both the near-wellbore and deep damage in sandstone and carbonate reservoirs. Click on the "Module" dropdown menu and select "Matrix Acidizing". This will open the main data entry form. Each input data offers the choice for the unit used in data entry. By clicking on the arrow beside the unit, a dropdown menu will show the different units that could be used for this variable. The main input form has four tabs that include all of the input data needed by the

software to design the treatment. To move between tabs, select the required tab by clicking on its name at the top of the tab control box. The bottom of the form will direct the user to the missing data needed for the next step of the design. Once the data entry has satisfied the minimum requirement for this case, the "Design" button will be activated.

Reservoir Characteristics

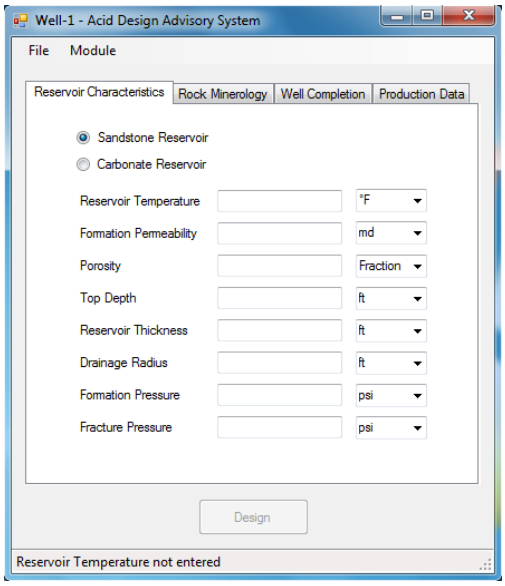

Figure 5.9 - Reservoir characteristics tab.

The reservoir characteristics tab contains different properties of the reservoir such as the permeability, porosity, depth, and thickness. This data could change depending on the data entered (e.g., in a case where horizontal well permeability could be entered as horizontal and vertical permeability). All data entered provides the choice of units based on the widely used unit systems. Numbers that have different units will

need to be manually converted to any of the units provided by the software prior to their entry.

Formation/Fracture Pressure: both the formation and fracture pressures could be entered in either the form of absolute pressure or pressure gradient (reference depth is assumed to be at the top of the reservoir).

Rock Mineralogy

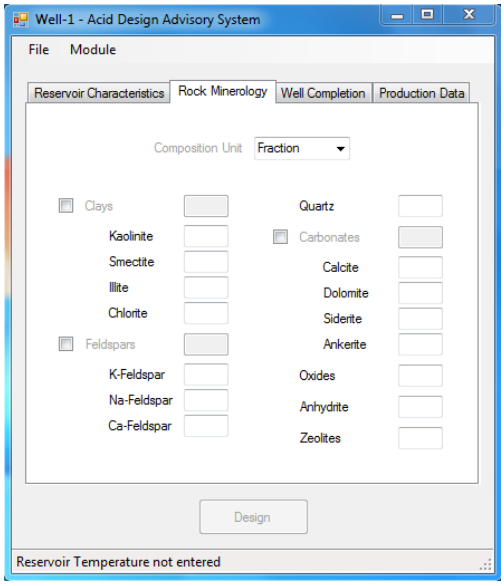

Figure 5.10 - Rock mineralogy tab.

The rock mineralogy tab is the tab for the composition of your rock. All entered compositions should be in the unit selected from the dropdown menu at the top of the tab. For clays, feldspars, and carbonates, the software gives the choice of either entering an overall composition or giving the composition of each component separately (i.e., for feldspars the user could choose to enter the feldspar content or the composition of each

of sodium, potassium, and calcium feldspars). This is done by clicking on the checkbox beside the "Clays", "Feldspars", or "Carbonates" labels.

Well Completion

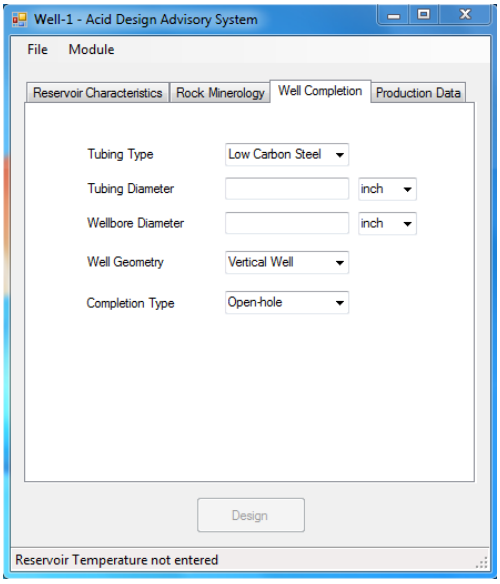

Figure 5.11 - Well completion tab.

The well completion tab allows the user to select the type of well geometry, type of completion, and the type of tubing used. Changing this data may change the data entry forms in other tabs and may change the data requirement for the proper acid design. An example of the effect of the data entered on this tab is the difference in the first tab (reservoir characteristics tab) between vertical or inclined wells from one side and the horizontal wells on the other side.

Production Data

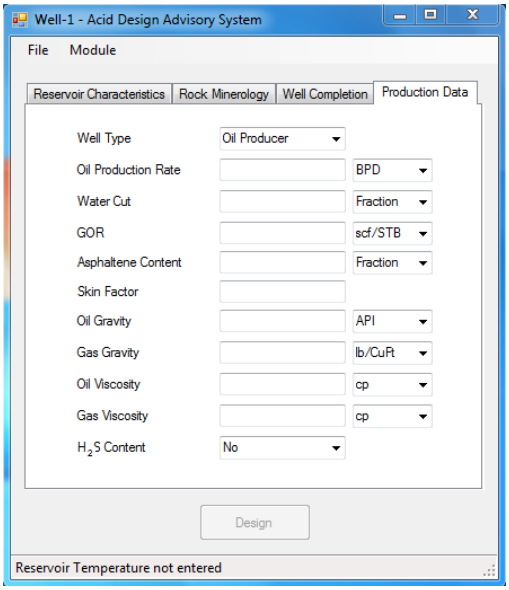

Figure 5.12 - Production data tab.

"Production Data" tab allows the entry of the production/injection data along with the fluid properties. By changing the type of well, the data entered will be changed accordingly to match the requirements for each case. In all data entered, the user can choose the units of the data.

Output Form

The output form contains three main sections. The first section identifies the well. The second section represents a summary for some of the main input data used in the design, including the temperature, type of rock, and mineralogy. This helps compare treatment designs with wells having similar properties to literature. The third part represents the proposed treatment and is used for output of designs calculated by the software.

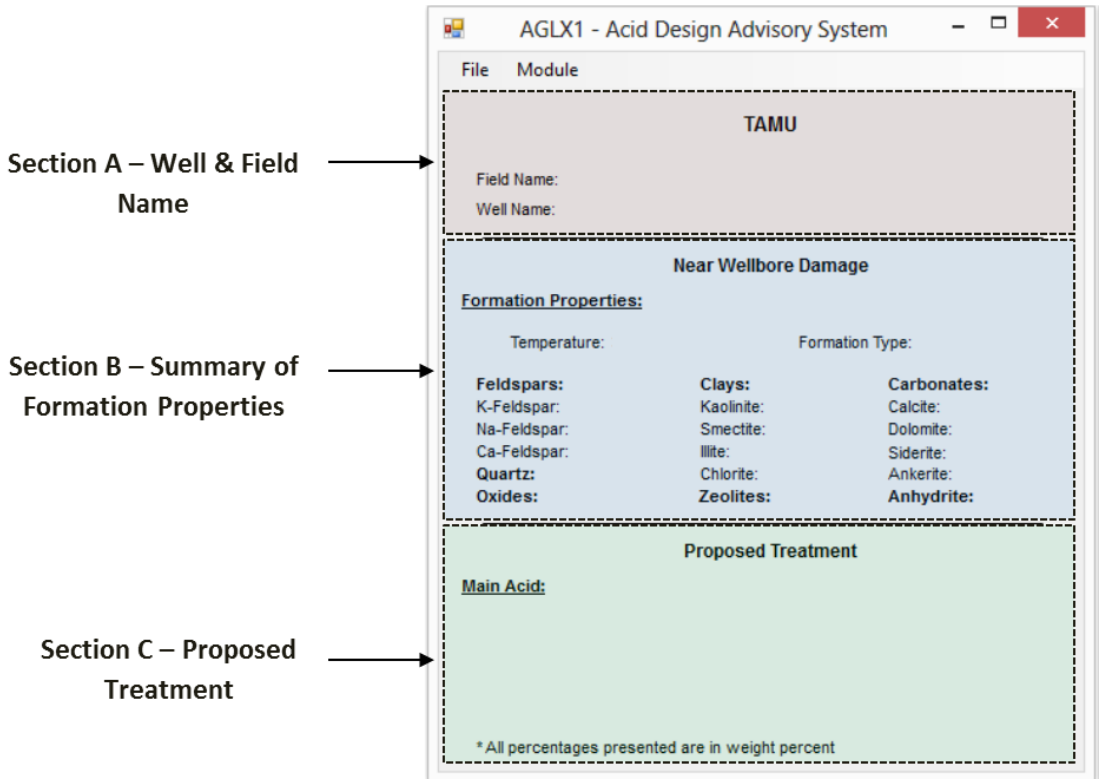

Figure 5.13 - Output form.

CHAPTER VI

CONCLUSIONS AND RECOMMENDATIONS

Among the most important concepts from previous guidelines, aside from the experimental work done, is that sandstone formations with carbonate content of higher than 15 or 20% should be treated by the same method as treating carbonate rocks. This was first mentioned by McLeod where he excluded sandstones with HCl solubility (carbonates) of higher than 20% and recommended using just HCl for their treatment. Later in 1999, Coulter and Jennings recommended treating sandstones with carbonate content of 15 to 20%. This hypothesis was proven to be valid in the experiments done with Bandera sandstones. Despite the expected damage resulting from the high Illite content of Bandera rock, HCl was capable of fairly enhancing the permeability of the cores. This was illustrated by the experiment with 0% HF where a permeability ratio of 1.9 was achieved. This enhancement was even more than that achieved using 2.5 and 3% HF.

By trying six different concentrations of HF for acidizing Bandera sandstone cores, it was clear from the experimental study that mud acid with 1 wt% HF was able to best enhance the permeability of the cores.

When four different concentrations of HF were attempted for acidizing Grey Berea sandstone cores it was clear from the experimental study that mud acid with an HF concentration of 1.8 wt% would achieve the best results.

The mineralogy of the reservoir is the most significant factor in designing the sandstone acid treatment.

REFERENCES

Averill, B.A. and Eldredge, P. 2006. General Chemistry: Principles, Patterns, and Applications. In, ed. Averill, B., 2. Ontario, Canada: Pearson Education Canada. 0805383190 / 0-8053-8319-0

Chiu, T.-J., Caudell, E.A., and Wu, F.-L. 1993. Development of an Expert System to Assist with Complex Fluid Design. SPE Computer Applications 5 (1): 18-20. 00024416.

Coulter, G.R. and Jennings, A.R., Jr. 1999. A Contemporary Approach to Matrix Acidizing. SPE Production & Operations 14 (2): 144-149. SPE-056279.

Economides, M.J. and Nolte, K.G. 2000. Reservoir Stimulation. eds. Economides, M.J. and Nolte, K.G. Chichester, England, New York Wiley.

Gdanski, R. 1998. Kinetics of Tertiary Reactions of Hydrofluoric Acid on Aluminosilicates. SPE Production & Operations 13 (2): 75-80. 00031076.

Gdanski, R. 1999. Kinetics of the Secondary Reaction of Hf on Alumino-Silicates. SPE Production & Operations 14 (4): 260-268. 00059094.

Hartman, R.L., Lecerf, B., Frenier, W.W. et al. 2006. Acid-Sensitive Aluminosilicates: Dissolution Kinetics and Fluid Selection for Matrix-Stimulation Treatments. SPE Production & Operations 21 (2): pp. 194-204. SPE-82267-PA.

Kalfayan, L. 2008. Production Enhancement with Acid Stimulation. 2nd edition. Tulsa, Oklahoma: PennWell.

McLeod, H.O., Ledlow, L.B., and Till, M.V. 1983. The Planning, Execution, and Evaluation of Acid Treatments in Sandstone Formations. Paper presented at the SPE Annual Technical Conference and Exhibition, San Francisco, California. SPE SPE-011931.

McLeod, H.O. 1984. Matrix Acidizing. Journal of Petroleum Technology 36 (12): 2055-2069. 00013752.

McLeod, H.O. 1989. Significant Factors for Successful Matrix Acidizing. Paper presented at the SPE Centennial Symposium at New Mexico Tech, Socorro, New Mexico. SPE SPE-020155.

McLeod, H.O., Jr. and Norman, W.D. 2000. Sandstone Acidizing. In Reservoir Stimulation, ed. Economides, M.J. and Nolte, K.G., Chichester, UK: John Wiley and Sons.

Nitters, G., Roodhart, L., Jongma, H. et al. 2000. Structured Approach to Advanced Candidate Selection and Treatment Design of Stimulation Treatments. Paper presented at the SPE Annual Technical Conference and Exhibition, Dallas, Texas. SPE SPE-063179-ms.

Shaughnessy, C.M. and Kunze, K.R. 1981. Understanding Sandstone Acidizing Leads to Improved Field Practices. Journal of Petroleum Technology 33 (7): 1196-1202. SPE-009388-PA.

Shuchart, C.E. and Gdanski, R.D. 1996. Improved Success in Acid Stimulations with a New Organic-Hf System. Paper presented at the European Petroleum Conference, Milan, Italy. SPE SPE-036907.

Simon, D.E. and Anderson, M.S. 1990. Stability of Clay Minerals in Acid. Paper presented at the SPE Formation Damage Control Symposium, Lafayette, Louisiana. SPE 00019422.

Smith, C.F. and Hendrickson, A.R. 1965. Hydrofluoric Acid Stimulation of Sandstone Reservoirs. Journal of Petroleum Technology 17(2): 215-222.

Walker, M.L., Dill, W.R., Besler, M.R., and McFatridge, D.G. 1991. Iron Control in West Texas Sour-Gas Wells Provides Sustained Production Increases. SPE Journal of Petroleum Technology 43 (5): 603-607.

Walsh, M.P., Lake, L.W., and Schechter, R.S. 1982. A Description of Chemical Precipitation Mechanisms and Their Role in Formation Damage During Stimulation by Hydrofluoric Acid. Journal of Petroleum Technology 34 (9): 2097-2112. 00010625.

Williams, B.B., Gidley, J.L., and Schechter, R.S. 1979. Acidizing Fundamentals. Monograph / Society of Petroleum Engineers of AIME. Monograph ;V. 6 Henry L. Doherty Series. New York Henry L. Doherty Memorial Fund of AIME, Society of Petroleum Engineers of AIME.

Wilson, M.D. 1982. Origins of Clays Controlling Permeability in Tight Gas Sands. Journal of Petroleum Technology 34 (12): 2871-2876. 00009843.